

# **$G_2$ Holonomy, Mirror Symmetry and Phases of $N=1$ SYM**

Kazuo Hosomichi and David C. Page

*Department of Physics, University of Toronto,  
60 St. George Street, Toronto, Ontario M5S 1A7, Canada*

## **Abstract**

We study the phase structure of four-dimensional  $\mathcal{N} = 1$  super Yang-Mills theories realized on D6-branes wrapping the  $\mathbb{RP}^3$  of a  $\mathbb{Z}_2$  orbifold of the deformed conifold. The non-trivial fundamental group of  $\mathbb{RP}^3$  allows for the gauge group to be broken to various product groups by  $\mathbb{Z}_2$  Wilson lines. We study the classical moduli space of theories in various pictures related by dualities including an M-theory lift. The quantum moduli space is analyzed in a dual IIB theory, where a complex curve contained in the target space plays a key role. We find that the quantum moduli space is made up of several branches, characterized by the presence or absence of a low energy  $U(1)$  gauge symmetry, which are connected at points of monopole condensation. The resulting picture of the quantum moduli space shows how the various gauge theories with different product gauge groups are connected to one another.

## 1. Introduction

Understanding the dynamics of string compactifications to four dimensions with  $\mathcal{N} = 1$  supersymmetry is one of the most important challenges confronting string theory. A better understanding of this subject is necessary in order to learn more about the vacuum structure of string theory and will be crucial for connecting to real world physics. One problem of fundamental interest is to understand the structure of the moduli space of  $\mathcal{N} = 1$  string backgrounds and we shall study a particular example of this in the current work.

One fruitful example, which has been studied by a number of authors, is the case of the geometric transition for type II strings compactified on the conifold in the presence of branes and flux. This study was initiated in [1] (following earlier work on topological strings [2]), in which the open-closed string duality involving D6-branes wrapping the minimal  $S^3$  of the deformed conifold

$$z_1^2 + z_2^2 + z_3^2 + z_4^2 = \mu, \quad (1.1)$$

was related to the dynamics of  $\mathcal{N} = 1$  pure SYM theory. A large number of D6-branes bring the geometry into a resolved conifold with RR2-form flux. String theory relates the SYM scale  $\Lambda$  with the volume of  $S^3$  and the gaugino condensate  $S$  with the volume of the blown-up  $S^2$ , and the relation between the deformed and resolved conifolds gives a precise relation between  $\Lambda$  and  $S$ .

This smooth geometric transition of the conifold was understood from the M-theory viewpoint in [3, 4, 5]. For  $SU(N)$  SYM theory, it was shown that the compactification manifold should be a  $\mathbb{Z}_N$  orbifold of  $\mathbb{R}^4 \times S^3$  with metric of  $G_2$  holonomy,

$$ds^2 = \frac{dr^2}{1 - (r_0/r)^3} + \frac{r^2}{36}(1 - (r_0/r)^3) \sum_{a=1}^3 (\sigma_a + \tilde{\sigma}_a)^2 + \frac{r^2}{12} \sum_{a=1}^3 (\sigma_a - \tilde{\sigma}_a)^2. \quad (1.2)$$

Here  $r_0$  denotes the unique non-normalizable deformation of the background, and  $\sigma_a$  and  $\tilde{\sigma}_a$  are two sets of  $SU(2)$  Maurer-Cartan 1-forms. As was discussed in [5], the classical moduli space of  $G_2$  holonomy manifolds  $\mathbb{R}^4 \times S^3$  consists of three half-lines emanating from a point. This can be understood as follows. We regard the space as a deformation of a cone over

$$S^3 \times S^3 \cong SU(2)^3 / SU(2) \equiv \{(g_1, g_2, g_3) \sim (g_1 h, g_2 h, g_3 h) \mid g_{1,2,3}, h \in SU(2)\}. \quad (1.3)$$

The three branches of classical moduli space correspond to the three choices of  $S^3 - g_1, g_2$  or  $g_3$  – to fill in in order to make the  $\mathbb{R}^4$ . On one branch, the  $\mathbb{Z}_N$  acts on the  $\mathbb{R}^4$  part and has an  $S^3$  fixed point locus, leading to  $SU(N)$  gauge dynamics, whereas on the other two branches, the  $\mathbb{Z}_N$  acts freely and there is no gauge dynamics.

Including the modulus corresponding to the M-theory three-form potential through  $S^3$ , the moduli space is complex one-dimensional and classically is given by three semi-infinite cylinders meeting at a point. Quantum effects turn this into a single smooth quantum moduli space which is a Riemann sphere with three semi-classical (large volume) points. This quantum moduli space was shown to encode the dynamics of the SYM theory (with some higher order corrections) such as the relation between  $\Lambda$  and  $S$  mentioned above. Note that the Riemann sphere contains the vacua corresponding to different  $\Lambda$ , so it should better be called the moduli space of vacua and theories.

Through the analysis of various orbifold groups, [5] also showed that two gauge theories with different microscopic gauge groups can sometimes appear on the same string theory moduli space. One example is the case of the orbifold of  $\mathbb{R}^4 \times S^3$  by the dihedral group  $D_{4+n}$ , where two SYM theories with gauge groups  $SO(2n+8)$  and  $Sp(n)$  are connected on the same moduli space. As another example, [6] studied more complicated orbifold groups of the form  $\Gamma = \Gamma_1 \times \Gamma_2 \times \Gamma_3$  which, among other things, give rise to the possibility for the gauge groups to be broken by discrete Wilson lines (see also [7]).

An example of this kind is the orbifold  $(\mathbb{R}^4/\mathbb{Z}_N) \times (S^3/\mathbb{Z}_2)$  corresponding to  $N$  D6-branes on a  $\mathbb{Z}_2$  orbifold of conifold, and this is the model which we will focus on in this paper. Since one has a choice of  $\mathbb{Z}_2$  Wilson line  $\pi_1(S^3/\mathbb{Z}_2) \rightarrow SU(N)$ , there arise backgrounds corresponding to various classical gauge groups  $U(1) \times SU(N_+) \times SU(N_-)$  with  $N_+ + N_- = N$ . One can then ask how all these backgrounds are put together to form a quantum moduli space. A recent related work [8, 9] has obtained, in a different setting, smooth moduli spaces that interpolate between vacua of SYM theories with different classical gauge groups.

It has recently been conjectured that the  $U(N)$  Chern-Simons theory on  $\mathbb{RP}^3$  is dual to the closed topological A-model on a non-compact Calabi-Yau manifold  $\mathcal{O}(K) \rightarrow \mathbb{P}^1 \times \mathbb{P}^1$  [1, 10, 11], and the corresponding large  $N$  duality is expected to hold also in superstring theory. On the Chern-Simons side, there is a choice of  $\mathbb{Z}_2$  Wilson line which breaks the gauge group to product groups. The numbers  $N_+, N_-$  appear on the closed string side as the sizes of two  $\mathbb{P}^1$ 's and are also proportional to the RR2-form flux piercing through them. By analogy with the story for the conifold, one expects that this resolved geometry describes the low energy dynamics of SYM theories with these product gauge groups.

The aim of this paper is to obtain the phase structure of four-dimensional string compactifications which are on the same  $\mathcal{N} = 1$  moduli space as the background with  $N$  D6-branes wrapping the minimal  $\mathbb{RP}^3$  of a  $\mathbb{Z}_2$  orbifold of the deformed conifold. We will first study the classical moduli space by listing the classical solutions or brane configurations with the same asymptotic boundary conditions in a given string or M-theory setup, and then move on to a study of the quantum moduli space.

The analysis will be made from several frameworks related by a chain of dualities. As

was shown in [12, 5], D6-branes wrapped on the  $S^3$  of the deformed conifold are dual, via an M-theory lift, to a configuration of a Lagrangian D6-branes on an orbifold of  $\mathbb{C}^3$ , which admits a gauged linear sigma model description. This also has a mirror IIB description in terms of D5-branes on a non-compact Calabi-Yau. We will find the IIB framework to be the most powerful for analyzing the quantum moduli space. Finally, there is a duality to three-dimensional webs of 5-branes in IIB string theory which offers a particularly useful description of the classical moduli space.

This paper is organized as follows. In section 2 we describe our problem and discuss the classical moduli space in the original type IIA setting. It is up-lifted to M-theory in section 3, where we explain the various  $G_2$  holonomy spaces corresponding to branches of classical moduli space. In addition to orbifolds of the  $\mathbb{R}^4 \times S^3$  geometry explained above, we will need different  $G_2$  holonomy solutions with the same asymptotics and a minimal  $T^{p,q}$  at the center. In section 4 we dimensionally reduce to another IIA picture and obtain a description of the classical moduli space in terms of a gauged linear sigma model. Various  $G_2$  holonomy manifolds are mapped to configurations of a D6-brane in different partial blow-ups of a toric orbifold  $\mathbb{C}^3/(\mathbb{Z}_N \times \mathbb{Z}_2)$ . Also, in sections 3,4 we explain another type IIB dual in which these classical vacua are described as three-dimensional webs of 5-branes with fixed asymptotics. We will make use of these webs to prove that there are no further classical vacua with the required asymptotics. Finally, in section 5 we take the mirror of the GLSM and move to a IIB theory on a non-compact Calabi-Yau space containing a complex curve  $\Sigma$ . The D6-brane of the IIA theory turns into a non-compact D5-brane intersecting with  $\Sigma$  at a point. The presence of this brane generates a superpotential  $W$  for the closed string moduli. By a careful analysis of  $\Sigma$  and  $W$  we will obtain the branch structure of the quantum moduli space. This moduli space will turn out to interpolate between various SYM theories with different product gauge groups.

## 2. Classical phases of the type IIA geometry

We are interested in a  $\mathbb{Z}_2$  orbifold of the deformed conifold (1.1), where  $\mathbb{Z}_2$  acts as  $z_i \rightarrow -z_i$ . Acting on the deformed conifold, the  $\mathbb{Z}_2$  is fixed point free and the minimal  $S^3$  becomes an  $\mathbb{RP}^3$ . Indeed the orbifold space is topologically (and symplectically)  $T^*\mathbb{RP}^3$ .

We wish to consider  $N$  D6-branes wrapping the base  $\mathbb{RP}^3$ . Naively we would expect to find a  $U(N)$  gauge theory living on the worldvolume of the D-branes. On lifting to M-theory, we find an  $SU(N)$  gauge group as discussed in [13] and reviewed in the next section. We can also see this within the IIA setup as the resolved conifold does not have a normalizable harmonic two-form and thus the  $U(1)$  is missing after geometric transition. We shall assume that the  $SU(N)$  gauge group is correct although we do not understand

the mechanism for removing the extra  $U(1)$  in the D6-brane theory.

Note that this  $SU(N)$  gauge theory has many more vacua than the case without orbifold, since we can include Wilson lines  $\pi_1(\mathbb{RP}^3) \cong \mathbb{Z}_2 \rightarrow SU(N)$  which break the gauge group to  $SU(N_+) \times SU(N_-) \times U(1)$ . If  $N_-$  labels the number of  $(-1)$  eigenvalues of the Wilson line, then  $N_-$  is necessarily even, since the gauge group is  $SU(N)$  not  $U(N)$ . All this suggests a richer structure for the moduli space than in the case of the conifold.

Other semi-classical limits of moduli space should be described by geometries which are asymptotic to a cone over  $T^{1,1}/\mathbb{Z}_2$  with  $N$  units of RR-flux through the  $S^2$ . One possibility is the  $\mathbb{Z}_2$  orbifold of the resolved conifold. In this case, the  $\mathbb{Z}_2$  has a  $\mathbb{P}^1$  of fixed points and we can consider blowing up the singularity to form a space with two non-trivial  $\mathbb{P}^1$ 's. The blown up space is  $\mathcal{O}(K) \rightarrow \mathbb{P}^1 \times \mathbb{P}^1$ .

This geometry has two Kähler parameters. The first is related to an overall rescaling of the metric whilst the other controls the relative size of the two  $\mathbb{P}^1$ 's. The overall rescaling is a non-normalizable parameter labelling different points on the moduli space of theories. The relative rescaling of the two  $\mathbb{P}^1$ 's is normalizable and corresponds to a dynamical field, which gets frozen by a flux superpotential. The value at which it gets frozen depends on the background RR-flux.

In fact it is possible to be completely explicit here. The Calabi-Yau metric on  $\mathcal{O}(K) \rightarrow \mathbb{P}^1 \times \mathbb{P}^1$  was found in [14]. It is<sup>1</sup>:

$$ds^2 = \kappa^{-1}(\rho)d\rho^2 + \frac{1}{9}\kappa(\rho)\rho^2(\sigma_3 - \tilde{\sigma}_3)^2 + \frac{1}{6}\rho^2(\sigma_1^2 + \sigma_2^2) + \frac{1}{6}(\rho^2 + 6a^2)(\tilde{\sigma}_1^2 + \tilde{\sigma}_2^2), \quad (2.1)$$

where

$$\kappa(\rho) = \frac{1 + \frac{9a^2}{\rho^2} - \frac{b^6}{\rho^6}}{1 + \frac{6a^2}{\rho^2}} \quad (2.2)$$

and  $a$  and  $b$  are parameters. Varying  $a$  is a non-normalizable deformation whilst varying  $b$  is normalizable.

As in the introduction  $\sigma_a, \tilde{\sigma}_a$  are two sets of  $SU(2)$  Maurer-Cartan forms. Explicitly,  $X^{-1}dX = \frac{i}{2}\tau_a\sigma_a$  where  $\tau_a$  are Pauli's matrices,

$$X = \begin{pmatrix} \cos \frac{\theta}{2} e^{\frac{i}{2}(\psi+\phi)} & -\sin \frac{\theta}{2} e^{-\frac{i}{2}(\psi-\phi)} \\ \sin \frac{\theta}{2} e^{\frac{i}{2}(\psi-\phi)} & \cos \frac{\theta}{2} e^{-\frac{i}{2}(\psi+\phi)} \end{pmatrix} \quad (0 \leq \psi < 4\pi, \quad 0 \leq \phi < 2\pi, \quad 0 \leq \theta < \pi) \quad (2.3)$$

and  $\tilde{X}(\tilde{\psi}, \tilde{\theta}, \tilde{\phi})$  and  $\tilde{\sigma}_a$  are defined similarly. The radial coordinate  $\rho \in [\rho_0, \infty)$  where  $\rho_0$  is defined as the positive value of  $\rho$  at which  $\kappa(\rho)$  vanishes. In order to remove a conical singularity at this locus, it is necessary to orbifold by  $\mathbb{Z}_2$  so that  $\check{\psi} = \psi - \tilde{\psi}$  has length  $2\pi$ . At  $\rho \rightarrow \infty$  the metric approaches the standard metric on (the  $\mathbb{Z}_2$  orbifold of) the conifold.

---

<sup>1</sup>Although the metric is written in terms of seven independent coordinates, it depends on  $\psi, \tilde{\psi}$  (introduced below) only through  $\psi - \tilde{\psi}$ .

The Kähler form corresponding to this choice of metric is:

$$\omega_0 = \frac{1}{3}\rho d\rho \wedge (\sigma_3 - \tilde{\sigma}_3) + \frac{1}{6}\rho^2 \sigma_1 \wedge \sigma_2 - \frac{1}{6}(\rho^2 + 6a^2)\tilde{\sigma}_1 \wedge \tilde{\sigma}_2. \quad (2.4)$$

We should allow fluctuations of the Kähler class by elements of normalizable second cohomology. There is one such class, which is generated by the two-form:

$$\omega_1 = d(u(\rho)(\sigma_3 - \tilde{\sigma}_3)) = \frac{\partial u}{\partial \rho} d\rho \wedge (\sigma_3 - \tilde{\sigma}_3) + u(\sigma_1 \wedge \sigma_2 - \tilde{\sigma}_1 \wedge \tilde{\sigma}_2), \quad (2.5)$$

where  $u$  is an arbitrary function of  $\rho$  which approaches a constant  $u_0$  at  $\rho = \rho_0$  and dies away faster than  $1/\rho$  at  $\rho \rightarrow \infty$ .  $\omega_1$  is harmonic for the special choice

$$u = \frac{1}{\rho^2(\rho^2 + 6a^2)}. \quad (2.6)$$

In order to measure the correct RR two-form flux at infinity, we need to fix the non-normalizable component of the flux. The condition is that the total flux through both  $\mathbb{P}^1$ 's is  $N$  units:

$$F|_{\rho \rightarrow \infty} = \frac{N}{2} (\sigma_1 \sigma_2 + \tilde{\sigma}_1 \tilde{\sigma}_2) + \dots \quad (2.7)$$

The different ways of partitioning this flux between the two  $\mathbb{P}^1$ 's cannot be distinguished at infinity since we can change this partitioning by adding a suitable multiple of  $\omega_1$  to  $F$ . All partitions into a pair of integers  $(N_+, N_-)$  appear to give possible semi-classical branches of moduli space:

$$F|_{\rho=\rho_0} = N_+ \sigma_1 \sigma_2 + N_- \tilde{\sigma}_1 \tilde{\sigma}_2. \quad (2.8)$$

In fact, we should be careful here. A close consideration of the way in which the orbifold group acts on the total space of the  $U(1)$  fibre bundle reveals that the cases with  $N_-$  even or odd can be distinguished at infinity. We shall postpone a discussion of this subtlety until the next section in which we lift to M-theory.

After fixing a choice of partition, a flux superpotential is generated for the normalizable Kähler parameter. At large volume, this flux superpotential is:

$$g_s W = \int F \wedge \omega \wedge \omega = \int F \wedge (\omega_0 + \chi \omega_1) \wedge (\omega_0 + \chi \omega_1). \quad (2.9)$$

$F$  is quantized and thus provides a fixed background whilst  $\chi$  is a fluctuating field. The vacuum equations are:

$$\partial_\chi W = \frac{2}{g_s} \int F \wedge (\omega_0 + \chi \omega_1) \wedge \omega_1 = 0. \quad (2.10)$$

Using the expression (2.5) for  $\omega_1$  we can integrate (2.10) using Stokes' theorem to find boundary contributions at  $\rho = \rho_0$  and  $\infty$ . The contribution at  $\rho = \infty$  vanishes whilst the contribution at  $\rho = \rho_0$  vanishes if  $\chi$  is fixed so that:

$$\omega|_{\rho=\rho_0} \propto (N_+ \sigma_1 \sigma_2 - N_- \tilde{\sigma}_1 \tilde{\sigma}_2). \quad (2.11)$$

Thus the vacuum equations imply that the relative sizes of the two  $\mathbb{P}^1$ 's are directly proportional to the fluxes through them. We will find confirmation of this result when we lift to M-theory in the following section.

In summary, we have found that in addition to the deformed conifold branches, there is a collection of  $O(K) \rightarrow \mathbb{P}^1 \times \mathbb{P}^1$  branches labelled by two integers  $(N_+, N_-)$  corresponding to the fluxes through the two  $\mathbb{P}^1$ 's. Each of these branches is a (complex) one-dimensional family of backgrounds, parametrized locally by the value of the non-normalizable Kähler modulus. Furthermore, each background has a unique vacuum state since the normalizable parameter is frozen. There is a massless  $U(1)$  field in each of the  $O(K) \rightarrow \mathbb{P}^1 \times \mathbb{P}^1$  backgrounds, since no mass term is generated for the vector field in the same  $\mathcal{N} = 2$  multiplet as  $\chi$ .

### 3. M-theory lift

Next we lift the various families of solutions to M-theory. We shall find that the orbifolds of the deformed and resolved conifolds lift to orbifolds of the  $G_2$  manifold  $\mathbb{R}^4 \times S^3$  described in the introduction whilst the solutions with local  $\mathbb{P}^1 \times \mathbb{P}^1$  lift to a new class of  $G_2$  manifolds found in [15]. These are all the solutions of  $G_2$  holonomy which asymptote to a unique  $G_2$  cone over  $S^3/\mathbb{Z}_2 \times S^3/\mathbb{Z}_N$  as we shall argue later using a 5-brane web analysis.

Each solution is labelled by the size of the minimal cycle in the interior together with a 3-form period integral, and we recover the unique  $G_2$  cone in the limit of vanishing cycle. Therefore, the classical moduli space consists of several (complex) one-dimensional branches all meeting at the singular cone. In discussing the modification of this picture due to quantum effects, the low energy gauge symmetry is an important characteristic of branches. The orbifolds of  $\mathbb{R}^4 \times S^3$  support no gauge symmetry, but the new solutions are expected to have one normalizable harmonic 2-form and support a  $U(1)$  gauge symmetry. We shall use the number of  $U(1)$  factors,  $g = 0$  or  $1$ , as a label of branches.

#### 3.1. $g = 0$ BRANCH

The configuration of  $N$  D6-branes wrapped on the  $\mathbb{RP}^3$  of the  $\mathbb{Z}_2$  orbifold of the deformed conifold lifts to an orbifold of the familiar  $G_2$  holonomy manifold of topology

$\mathbb{R}^4 \times S^3$ . In order to get  $N$  D6-branes we orbifold the  $\mathbb{R}^4$  by  $\mathbb{Z}_N$ . In addition we should orbifold by  $\mathbb{Z}_2$  in order to get an  $S_3/\mathbb{Z}_2$ . In the description in terms of  $(g_1, g_2, g_3) \sim (g_1 h, g_2 h, g_3 h)$  with  $g_1$  filled in to make an  $\mathbb{R}^4$ , we have  $\mathbb{Z}_2 \times \mathbb{Z}_N$  acting as:

$$(g_1, g_2, g_3) \sim (g_1, -g_2, g_3) \sim (\omega g_1, g_2, g_3) , \quad \omega^N = 1. \quad (3.1)$$

The classical moduli space has two more  $g = 0$  branches with  $g_2$  or  $g_3$  filled in. In the second branch where  $g_2$  is filled in, we have  $(\mathbb{R}^4/\mathbb{Z}_2) \times (S^3/\mathbb{Z}_N)$ , and the M-theory circle is identified with the Hopf fibre of  $\mathbb{Z}_N$  lens space. The IIA configuration is therefore a  $\mathbb{Z}_2$  orbifold of the resolved conifold with  $N$  flux turned on. The  $\mathbb{Z}_2$  reverses the four directions transverse to the  $\mathbb{P}^1$ , and the singularity supports an  $\mathcal{N} = 1$   $SU(2)$  SYM.

The classical geometry for the third branch with  $g_3$  filled in is the same as the second branch when  $N$  is even, but is different when  $N$  is odd. To see this, notice that in the gauge  $g_2 = 1$  the  $\mathbb{Z}_2$  acts on  $g_1$  and  $g_3$  as  $-1$  simultaneously. If  $N$  is even, one can redefine the generator of  $\mathbb{Z}_2$  by multiplying by the order two element of  $\mathbb{Z}_N$  so that it acts only on  $g_3$ . Thus the second and the third branches are identical in nature. On the other hand, for odd  $N$  one cannot do this redefinition, and moreover one can see that the  $\mathbb{Z}_2$  acts freely on the third branch. The resulting IIA geometry looks like the same  $\mathbb{Z}_2$  orbifold of the resolved conifold with  $N$  flux, but this time the  $\mathbb{Z}_2$  also acts on the M-theory circle as a half-period shift. So the  $\mathbb{Z}_2$  singularity does not support a gauge symmetry.

## Quantum moduli space

These three  $g = 0$  branches of classical moduli space are expected to form a single smooth  $g = 0$  branch of the quantum moduli space. Here we first briefly review the arguments of [5] for the case of  $\mathbb{R}^4 \times S^3$  without orbifold, and then discuss the case of our interest according to the analysis of [6].

The branch structure of classical solutions  $\mathbb{R}^4 \times S^3$  is conveniently described by the  $SU(2)$  matrices  $g_{1,2,3}$  obeying the equivalence relation (1.3). The three branches are obtained by filling in one of the  $g_i$  to make an  $\mathbb{R}^4$ .

Let  $\hat{D}_j$  denote the  $j$ -th copy of  $SU(2) \subset SU(2)^3$  and denote by  $D_j$  the 3-cycle in  $Y = SU(2)^3/SU(2)$  which is the projection of  $\hat{D}_j$  into  $Y$ . The  $D_j$  obey an homology relation

$$D_1 + D_2 + D_3 = 0.$$

Furthermore, in the  $j$ -th branch, the cycle  $D_j$  is trivial in homology, and  $Q_j = D_{j-1} = -D_{j+1}$  is non-vanishing. Define three holomorphic parameters  $\eta_{1,2,3}$  by

$$\eta_i = V(D_i), \quad V(D) \equiv \exp \left( - \int_D (\Phi + iC) \right)$$

using the harmonic 3-form  $\Phi$  and the 3-form potential  $C$ . They satisfy  $\eta_1\eta_2\eta_3 = -1$ , where the minus sign comes from a fermion anomaly [5]. Classically  $\eta_i = 1$ ,  $\eta_{i+1}\eta_{i-1} = -1$  on the  $i$ -th branch, but quantum mechanically all the three classical branches are on a single smooth Riemann sphere. Using the coordinate  $z$  such that the three large volume limits are corresponding to  $z = 0, 1, \infty$ , one finds

$$\eta_1 = 1 - z, \quad \eta_2 = \frac{1}{z}, \quad \eta_3 = \frac{z}{z-1}. \quad (3.2)$$

Let us then take the  $\mathbb{Z}_N \times \mathbb{Z}_2$  orbifold of this space, where the  $\mathbb{Z}_N$  and  $\mathbb{Z}_2$  of the orbifold group act on  $g_1$  and  $g_2$  from the left. By similar projections one finds the 3-cycles and the relation

$$D'_1 = S^3/\mathbb{Z}_N, \quad D'_2 = S^3/\mathbb{Z}_2, \quad D'_3 = \begin{cases} S^3/\mathbb{Z}_2, & \frac{N}{2}D'_1 + D'_2 + D'_3 = 0 \quad (N \text{ even}) \\ S^3, & ND'_1 + 2D'_2 + D'_3 = 0 \quad (N \text{ odd}) \end{cases}$$

The non-vanishing cycle in each branch is given by

$$Q'_1 = S^3/\mathbb{Z}_2, \quad Q'_2 = S^3/\mathbb{Z}_N, \quad Q'_3 = \begin{cases} S^3/\mathbb{Z}_N & (N \text{ even}) \\ S^3/\mathbb{Z}_{2N} & (N \text{ odd}) \end{cases} \quad (3.3)$$

Classically in branches 1,2,3 the cycles obey some homology relations as summarized in the table 1.

| $N$  | branch 1 ( $D'_1 = 0$ )      | branch 2 ( $D'_2 = 0$ )                | branch 3 ( $D'_3 = 0$ )                |
|------|------------------------------|--|--|
| even | $D'_2 = -Q'_1, D'_3 = Q'_1$  | $D'_3 = -\frac{N}{2}Q'_2, D'_1 = Q'_2$ | $D'_1 = -Q'_3, D'_2 = \frac{N}{2}Q'_3$ |
| odd  | $D'_2 = -Q'_1, D'_3 = 2Q'_1$ | $D'_3 = -NQ'_2, D'_1 = Q'_2$           | $D'_1 = -2Q'_3, D'_2 = NQ'_3$          |

Table 1: homology relations among various cycles.

The good local coordinates on the quantum moduli space around the three large volume points are the fractional instanton factors. For example on the first branch we have  $SU(N)$  gauge symmetry and so the fractional instanton factor is  $z_1 = V(Q'_1)^{1/N}$ . We define  $z_2$  and  $z_3$  similarly as the fractional instanton factors on the other two branches.

Defining  $\eta_i = V(D'_i)$  as before, one finds  $\eta_1^{N/2}\eta_2\eta_3 = 1$  for even  $N$  and  $\eta_1^N\eta_2^2\eta_3 = 1$  for odd  $N$ . Note that the sign must be determined from a careful analysis of the fermion anomaly, although we fix it by requiring consistency with the parametric representation of  $\eta_i$  given below. Near the three large-volume points the  $\eta_i$  behave as follows;

| $N$ even | $z_1 \sim 0$ | $z_2 \sim 0$ | $z_3 \sim 0$ | $N$ odd  | $z_1 \sim 0$ | $z_2 \sim 0$ | $z_3 \sim 0$ |
|----------|--------------|--------------|--------------|----------|--------------|--------------|--------------|
| $\eta_1$ | 1            | $z_2^2$      | $z_3^{-2}$   | $\eta_1$ | 1            | $z_2^2$      | $z_3^{-2}$   |
| $\eta_2$ | $z_1^{-N}$   | 1            | $z_3^N$      | $\eta_2$ | $z_1^{-N}$   | 1            | $z_3^N$      |
| $\eta_3$ | $z_1^N$      | $z_2^{-N}$   | 1            | $\eta_3$ | $z_1^{2N}$   | $z_2^{-2N}$  | 1            |

Assuming that the  $g = 0$  branch of the quantum moduli space is topologically a sphere and introducing the coordinate  $z$  as before, one finds  $\eta_i$  are expressed as the following functions of  $z$ :

$$\eta_1 = (1 - z)^2, \quad \eta_2 = z^{-N}, \quad \eta_3 = \begin{cases} z^N / (1 - z)^N & (N \text{ even}) \\ z^{2N} / (1 - z)^{2N} & (N \text{ odd}). \end{cases} \quad (3.4)$$

One is thus lead to the  $g = 0$  branch of quantum moduli space as in figure 1.

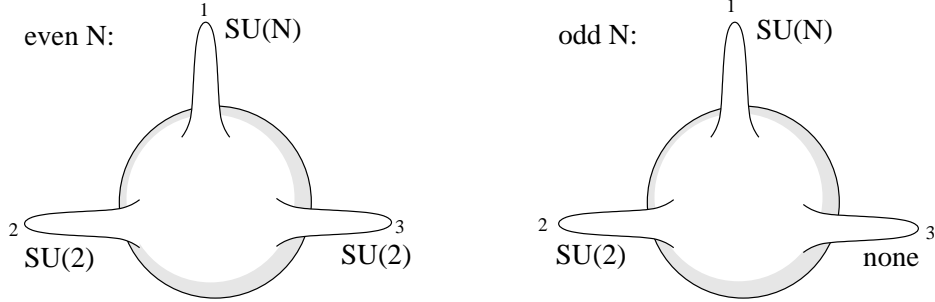


Figure 1:  $g = 0$  branch of quantum moduli space.

In the above we claimed that the orbifold of  $\mathbb{R}^4 \times S^3$  supports  $SU$  type gauge symmetries at various asymptotic regions of moduli space, and in particular there is no  $U(1)$  factor. Indeed, such a  $U(1)$  would arise from the M-theory 3-form dimensionally reduced along a normalizable harmonic 2-form on the  $G_2$  space, but there is no such 2-form even after the asymptotic behavior of the metric is modified so that there is an M-theory circle of finite radius at infinity [13]. This supports our earlier claim that the correct choice of gauge theory on the D-branes should be  $SU(N)$  rather than  $U(N)$ .

### 3.2. $g = 1$ BRANCHES

In this subsection we introduce a class of  $G_2$  holonomy metrics found in [15]. We claim that these solutions (with a suitable orbifold action) represent the M-theory lift of the IIA geometry with local  $\mathbb{P}^1 \times \mathbb{P}^1$ . They take the form:

$$ds^2 = dr^2 + a^2((\sigma_1 + h\tilde{\sigma}_1)^2 + (\sigma_2 + h\tilde{\sigma}_2)^2) + b^2(\tilde{\sigma}_1^2 + \tilde{\sigma}_2^2) + c^2(\sigma_3 - \tilde{\sigma}_3)^2 + f^2(\sigma_3 + h_3\tilde{\sigma}_3)^2 \quad (3.5)$$

where  $a, b, c, f, h$  and  $h_3$  are functions of the radial coordinate  $r$ . The two sets of  $SU(2)$  Maurer-Cartan forms  $\sigma_a, \tilde{\sigma}_a$  and the related  $SU(2)$  matrices  $X(\psi, \theta, \phi), \tilde{X}(\tilde{\psi}, \tilde{\theta}, \tilde{\phi})$  were defined in section 2.

At large  $r$ , the metric asymptotes to the  $S^1$  bundle over the conifold

$$ds^2 \underset{\text{large } r}{\sim} dr^2 + \frac{r^2}{6}(\sigma_1^2 + \sigma_2^2 + \tilde{\sigma}_1^2 + \tilde{\sigma}_2^2) + \frac{r^2}{9}(\sigma_3 - \tilde{\sigma}_3)^2 + f_\infty^2(\sigma_3 + \tilde{\sigma}_3)^2. \quad (3.6)$$

At small  $r$  the coefficient functions behave as

$$\begin{aligned} a &= a_0 + \mathcal{O}(r^2), & c &= -r + \mathcal{O}(r^2), \\ b &= b_0 + \mathcal{O}(r^2), & h &= \frac{b_0 f_0}{2a_0^3} r + \mathcal{O}(r^2), \\ f &= f_0 + \mathcal{O}(r^2), & h_3 &= \frac{b_0^2}{a_0^2} + \mathcal{O}(r^2). \end{aligned} \quad (3.7)$$

We see that a single  $S^1$  shrinks at  $r = 0$  and in the IIA geometry, upon reducing along the M-theory circle, we have a  $\mathbb{P}^1 \times \mathbb{P}^1$  bolt. Together with the asymptotic behaviour at  $r = \infty$  this ensures that the IIA reduction is topologically  $\mathcal{O}(K) \rightarrow \mathbb{P}^1 \times \mathbb{P}^1$ . In the limit that we shrink the M-theory circle to zero size, the exact Calabi-Yau metrics (2.1) are recovered [15].

We need to introduce an orbifold action in order to avoid a conical singularity at  $r = 0$ . Let us write  $a_0^2 = \lambda n_+$ ,  $b_0^2 = \lambda n_-$  for some  $\lambda \in \mathbb{R}$  which we shall fix presently, and observe:

$$\begin{aligned} ds^2 \underset{r \sim 0}{\simeq} & dr^2 + r^2(d\psi - d\tilde{\psi} + \cos\theta d\phi - \cos\tilde{\theta} d\tilde{\phi})^2 \\ & + \frac{f_0^2}{n_+^2}(n_+ d\psi + n_- d\tilde{\psi} + n_+ \cos\theta d\phi + n_- \cos\tilde{\theta} d\tilde{\phi})^2 \\ & + ds_{S^2 \times S^2}^2(\text{depends only on } r, \theta, \phi, \tilde{\theta}, \tilde{\phi}, \psi - \tilde{\psi}) + \dots \end{aligned}$$

There will be a conical singularity unless the shrinking vector

$$v = \frac{1}{n} \left( n_- \frac{\partial}{\partial \psi} - n_+ \frac{\partial}{\partial \tilde{\psi}} \right), \quad n \equiv n_+ + n_-, \quad |v|^2 = r^2 \quad (3.8)$$

has period  $2\pi$ . To remove this singularity we must impose

$$(\psi, \tilde{\psi}) \sim (\psi, \tilde{\psi}) + \frac{2\pi}{n}(n_-, -n_+). \quad (3.9)$$

Note that, in order for this identification to be a finite orbifold action on  $S^3 \times S^3$ ,  $n_+/n_- = a_0^2/b_0^2$  has to be rational. We fix  $\lambda$  by requiring that  $(n_+, n_-)$  be a pair of relatively prime positive integers. The bolt at  $r = 0$  is the smooth space  $T^{n_+, n_-}$  which is defined as the set of  $(X, \tilde{X})$  subject to the identification

$$(X, \tilde{X}) \sim (X e^{i\alpha n_- \tau_3}, \tilde{X} e^{-i\alpha n_+ \tau_3}). \quad (3.10)$$

An equivalent definition of  $T^{n_+, n_-}$  is as the  $U(1)$  bundle over  $\mathbb{P}^1 \times \mathbb{P}^1$  with monopole numbers  $(n_+, n_-)$ . Note that the orbifold group contains the following element

$$(\psi, \tilde{\psi}) \sim (\psi, \tilde{\psi}) + \frac{4\pi}{n}(1, 1). \quad (3.11)$$

We may consider a further orbifold by

$$(\psi, \tilde{\psi}) \sim (\psi, \tilde{\psi}) + \frac{4\pi}{N}(1, 1), \quad N \equiv kn, (k \in \mathbb{Z}), \quad (3.12)$$

which does not lead to any new singularities. With this choice of orbifold group, the total D6-brane charge is  $N = kn_+ + kn_- \equiv N_+ + N_-$ . After dimensional reduction on the M-theory circle to type IIA on  $\mathcal{O}(K) \rightarrow \mathbb{P}^1 \times \mathbb{P}^1$  we get  $(N_+, N_-)$  units of RR flux through the two  $\mathbb{P}^1$ 's. At  $r = 0$  in the M-theory geometry, one has a non-vanishing  $\mathbb{Z}_k$  orbifold of  $T^{n+, n-}$  which is identified with  $T^{N_+, N_-}$  under its definition above.

The restriction that  $a_0^2/b_0^2$  be rational, which we have just related to flux quantization in IIA, ensures that we have a discrete set of one-parameter families of solution labelled by  $(\lambda; N_+, N_-)$ , rather than a continuous two-parameter family labelled by  $(a_0, b_0)$ . Also, note that the volumes of the  $\mathbb{P}^1$ 's in the IIA geometry, which can be read off from the  $G_2$  metric at  $r = 0$ , are proportional to the fluxes. This agrees with the results of our IIA analysis using a flux superpotential.

Since the action of the orbifold group on  $(X, \tilde{X})$  is

$$(X, \tilde{X}) \sim (X\omega^{N_-/2}, -\tilde{X}\omega^{N_-/2}) \sim (X\omega, \tilde{X}\omega); \quad \omega = e^{\frac{2\pi i}{N}\tau_3},$$

by using the relation  $X = g_3 g_1^{-1}$ ,  $\tilde{X} = g_2 g_1^{-1}$  one finds the action of orbifold on  $(g_1, g_2, g_3)$

$$(g_1, g_2, g_3) \sim (\omega^{-N_-/2} g_1, -g_2, g_3) \sim (\omega g_1, g_2, g_3); \quad \omega = e^{\frac{2\pi i}{N}\tau_3}. \quad (3.13)$$

The structure of the orbifold group depends on whether  $N_\pm$  are even or odd.

- (i) If  $N_\pm$  are both even and therefore  $N$  is even, the orbifold group is  $\mathbb{Z}_2 \times \mathbb{Z}_N$ . It contains a  $\mathbb{Z}_2 \times \mathbb{Z}_2$  subgroup, a generator of which acts on  $g_2$  as a sign flip and the other flips  $g_3$ . So the orbifold group is invariant under the permutation of  $g_2$  and  $g_3$ .
- (ii) If  $(N_+, N_-) = (\text{odd, even})$ , the orbifold group is  $\mathbb{Z}_2 \times \mathbb{Z}_N$  with  $\mathbb{Z}_2$  acting on  $g_2$ . Note that the orbifold group acts  $g_2, g_3$  in an asymmetric way. If  $(N_+, N_-) = (\text{even, odd})$ , then the orbifold group is the same but now  $\mathbb{Z}_2$  acts on  $g_3$ .
- (iii) If  $N_\pm$  are both odd, the orbifold group is  $\mathbb{Z}_{2N}$  generated by  $(\omega^{1/2}, -1, 1)$  or

$$(\omega^{1/2}, -1, 1)^{N+1} \simeq (\omega^{1/2}, 1, -1).$$

The orbifold group action is therefore symmetric under the permutation of  $g_2, g_3$ .

Note the subtle dependence of the orbifold group on whether  $N_\pm$  is even or odd. At fixed  $N$ , the solutions asymptote to two distinct orbifolds of the  $S^1$  bundle over the conifold depending on  $N_-$  modulo 2. The solutions with even  $N_-$  and those with odd  $N_-$  are therefore realizing two distinct classes of four-dimensional  $\mathcal{N} = 1$  theories. This ties in nicely with our assumption that there is no overall  $U(1)$  gauge symmetry. Recall that near the semiclassical point 1 of the quantum  $g = 0$  branch drawn in figure 1 we expect  $SU(N)$  gauge symmetry and not  $U(N)$ . If the  $\mathbb{Z}_2$  Wilson lines were taking values in  $U(N)$ , the eigenvalues would be  $\pm 1$ 's with no further restriction. Since instead they take values in  $SU(N)$  the number of negative eigenvalues must be even.

Let us hereafter restrict to solutions with even  $N_-$ . The orbifold group acting on the asymptotic geometry is then the same for all the allowed distributions  $N = N_+ + N_-$ , so we have to take all of them into account in the discussion of the moduli space. They all constitute  $g = 1$  branches of moduli space characterized by the existence of an infrared  $U(1)$  gauge symmetry.

### 3.3. $T^3$ REDUCTION AND A TYPE IIB DUAL

We wish to explain what can be learnt about the moduli space of  $G_2$  compactifications by making a Kaluza-Klein reduction on  $T^3$ . The resulting base manifold is  $\mathbb{R}^4$ , as we explain below, and all the topological information is contained in the details of how cycles of the three-torus shrink.

First, we consider the case of the  $G_2$  geometry of topology  $\mathbb{R}^4 \times S^3$  with no orbifold. Consider the  $U(1)^3$  symmetry group generated by:

$$\begin{aligned} (1, 0, 0) &: (e^{\frac{-i\alpha\tau_3}{2}} g_1, e^{\frac{i\alpha\tau_3}{2}} g_2, e^{\frac{i\alpha\tau_3}{2}} g_3), \quad (e^{\frac{i\alpha\tau_3}{2}} X e^{\frac{i\alpha\tau_3}{2}}, e^{\frac{i\alpha\tau_3}{2}} \tilde{X} e^{\frac{i\alpha\tau_3}{2}}), \\ (0, 1, 0) &: (e^{\frac{i\alpha\tau_3}{2}} g_1, e^{\frac{-i\alpha\tau_3}{2}} g_2, e^{\frac{i\alpha\tau_3}{2}} g_3), \quad (e^{\frac{i\alpha\tau_3}{2}} X e^{\frac{-i\alpha\tau_3}{2}}, e^{\frac{-i\alpha\tau_3}{2}} \tilde{X} e^{\frac{-i\alpha\tau_3}{2}}), \\ (0, 0, 1) &: (e^{\frac{i\alpha\tau_3}{2}} g_1, e^{\frac{i\alpha\tau_3}{2}} g_2, e^{\frac{-i\alpha\tau_3}{2}} g_3), \quad (e^{\frac{-i\alpha\tau_3}{2}} X e^{\frac{-i\alpha\tau_3}{2}}, e^{\frac{i\alpha\tau_3}{2}} \tilde{X} e^{\frac{-i\alpha\tau_3}{2}}). \end{aligned} \quad (3.14)$$

Note that each  $U(1)$  is normalized to have length  $2\pi$ , since

$$(-g_1, -g_2, -g_3) \sim (g_1, g_2, g_3). \quad (3.15)$$

Now consider the Kaluza-Klein reduction on this  $T^3$ . A rough argument that this leads to an  $\mathbb{R}^4$  base is as follows. At  $r \neq 0$  the  $U(1)^3$  action leaves fixed the coordinates  $(r, \theta, \tilde{\theta}, \psi - \tilde{\psi})$  whilst acting transitively on the others.  $\theta$  and  $\tilde{\theta}$  each run from 0 to  $\pi$  and so together form a disc. On the boundaries of the disc,  $(\{\theta = 0, \pi\} \cup \{\tilde{\theta} = 0, \pi\})$ , the  $\psi - \tilde{\psi}$  direction can also be gauged away and so there is an  $S^1$  fibred over the disc that shrinks at the boundaries. This gives an  $S^3$ . At  $r = 0$ , additional directions shrink. In Phase 1, for example, the only non-shrinking direction at  $r = 0$  is the  $\tilde{\theta}$  line interval. Concentric  $S^3$ 's shrinking onto a line interval at  $r = 0$  will lead to an  $\mathbb{R}^4$  base.

Later, when we consider the  $G_2$  manifold with local  $T^{N_+, N_-}$ , the discussion is much the same except that the space at  $r = 0$  is a two-disc spanned by  $(\theta, \tilde{\theta})$ . The base is a family of concentric  $S^3$ 's flattening onto a two-disc leading once more to  $\mathbb{R}^4$ .

Now we need to find which  $S^1$ 's shrink at special loci in the geometry. It is straightforward to see that only the following  $S^1$ 's can shrink at generic radii:

$$\begin{aligned} (1, 0, 0) &\leftrightarrow (\theta = \pi, \tilde{\theta} = \pi), \\ (0, 1, 0) &\leftrightarrow (\theta = 0, \tilde{\theta} = \pi), \\ (0, 0, 1) &\leftrightarrow (\theta = \pi, \tilde{\theta} = 0), \\ (1, 1, 1) &\leftrightarrow (\theta = 0, \tilde{\theta} = 0). \end{aligned} \quad (3.16)$$

To see that these cycles shrink, note that  $\tau_3$  commutes with  $X$  for  $\theta = 0$  and anticommutes for  $\theta = \pi$ . Additionally, at  $r = 0$ , an  $S^3$  shrinks and so additional  $S^1$ 's may vanish there. In the  $i$ -th classical branch  $g_i$  shrinks and so

$$\begin{aligned} (0, 1, 1) &\leftrightarrow r = 0 \text{ (branch 1),} \\ (1, 0, 1) &\leftrightarrow r = 0 \text{ (branch 2),} \\ (1, 1, 0) &\leftrightarrow r = 0 \text{ (branch 3).} \end{aligned} \tag{3.17}$$

We can now draw a diagram which represents this information. In each case, the degeneration locus is three dimensional and two of these dimensions lie within the  $T^3$  fibre. Thus we can project onto the  $\mathbb{R}^4$  base and draw the degeneration loci as lines. The degenerations which happen at arbitrary radius give semi-infinite lines, whilst the others give line segments. The way in which the lines end on each other can easily be read from the results above.

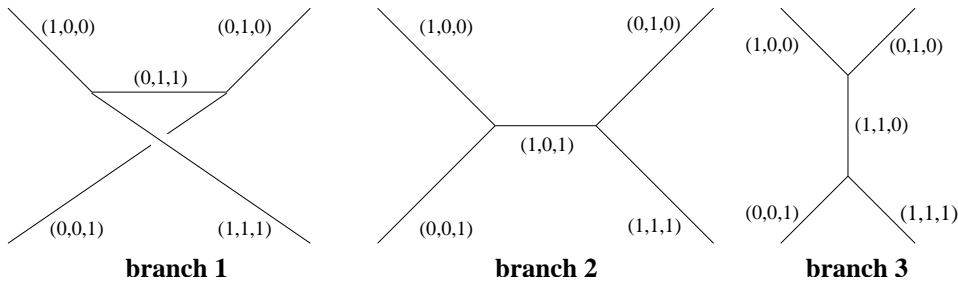


Figure 2: The three branches of the  $\mathbb{R}^4 \times S^3$  geometry

These graphs represent the three-branch structure of the classical moduli space of M-theory on  $\mathbb{R}^4 \times S^3$ . Each branch is parametrized by the the volume of the minimal  $S^3$  which is shown as the length of the internal leg.

As was discussed in [16, 12], by a chain of dualities we can relate these diagrams with three-dimensional webs of  $(p, q, r)$  5-branes in type IIB compactified on  $S^1 \times S^1 \times \mathbb{R}^4$ , where  $p, q$  denote the NS5-brane and D5-brane charges and  $r$  is the KK monopole charge along the first  $S^1$ .

In the case of a  $\mathbb{Z}_N$  orbifold acting on  $g_i$  as  $(g_1, g_2, g_3) \rightarrow (\omega g_1, g_2, g_3)$ ,  $\omega = e^{2\pi i \tau_3/N}$ , we should choose a different basis for our  $T^3$ . A suitable basis of 1-cycles of length  $2\pi$  is:

$$\begin{aligned} (1, 0, 0)' &: (e^{\frac{-i\alpha\tau_3}{2}} g_1, e^{\frac{i\alpha\tau_3}{2}} g_2, e^{\frac{i\alpha\tau_3}{2}} g_3), \\ (0, 1, 0)' &: (e^{\frac{i\alpha\tau_3}{2}} g_1, e^{\frac{-i\alpha\tau_3}{2}} g_2, e^{\frac{i\alpha\tau_3}{2}} g_3), \\ (0, 0, 1)' &: (e^{\frac{i\alpha\tau_3}{N}} g_1, g_2, g_3). \end{aligned} \tag{3.18}$$

The cycles that shrink at arbitrary radius are the same as before except that we need to take into account the change of basis. This amounts to rewriting in terms of the new

basis the labels of four semi-infinite legs

$$(1, 0, 0) = (1, 0, 0)', \quad (0, 1, 0) = (0, 1, 0)', \quad (0, 0, 1) = (0, -1, N)', \quad (1, 1, 1) = (1, 0, N)', \quad (3.19)$$

and those of the finite leg in each branch

$$(0, 1, 1) = N(0, 0, 1)', \quad (1, 0, 1) = (1, -1, N)', \quad (1, 1, 0) = (1, 1, 0'). \quad (3.20)$$

Interestingly, in the first branch the orbifold group has fixed points and this is reflected in the fact that the shrinking  $S^1$  at  $r = 0$  has length  $2\pi/N$ . Correspondingly there will be  $N$  coincident  $(0, 0, 1)$  5-branes at this locus in the  $(p, q, r)$  5-brane picture.

Let us now turn to the cases of our interest. First consider the geometries of  $g = 0$  given by  $\mathbb{Z}_N \times \mathbb{Z}_2$  orbifold of  $\mathbb{R}^4 \times S^3$ :

$$(g_1, g_2, g_3) \sim (g_1, -g_2, g_3) \sim (\omega g_1, g_2, g_3), \quad \omega = e^{2\pi i \tau_3/N}. \quad (3.21)$$

A suitable basis of cycles of length  $2\pi$  for the  $T^3$  is:

$$\begin{aligned} (1, 0, 0)'' &: (e^{\frac{i\alpha\tau_3}{N}} g_1, g_2, g_3), \\ (0, 1, 0)'' &: (g_1, e^{\frac{i\alpha\tau_3}{2}} g_2, g_3), \\ (0, 0, 1)'' &: (e^{\frac{i\alpha\tau_3}{2}} g_1, e^{\frac{i\alpha\tau_3}{2}} g_2, e^{\frac{-i\alpha\tau_3}{2}} g_3). \end{aligned} \quad (3.22)$$

The cycles which vanish at arbitrary radius are the same as in the previous examples (this statement is true on any branch of classical moduli space since it only depends on the asymptotic geometry). Moving to the new basis we make the replacements of the labels of external legs:

$$(1, 0, 0) = (0, 2, -1)'' , \quad (0, 1, 0) = (N, 0, -1)'' , \quad (0, 0, 1) = (0, 0, 1)'' , \quad (1, 1, 1) = (N, 2, -1)'' \quad (3.23)$$

and those of the internal legs

$$(0, 1, 1) = N(1, 0, 0)'' , \quad (1, 0, 1) = 2(0, 1, 0)'' , \quad (1, 1, 0) = \begin{cases} 2(N/2, 1, -1)'' & (N \text{ even}), \\ (N, 2, -2)'' & (N \text{ odd}). \end{cases} \quad (3.24)$$

The data of the fibre degenerations is summarized in figure 3 below.

Next consider the  $g = 1$  branches of the  $G_2$  geometry. In these branches, the following  $S^1$  shrinks at  $r = 0$ :

$$(X, \tilde{X}) \rightarrow (X e^{\frac{i\alpha\tau_3 N_-}{2N}}, \tilde{X} e^{\frac{-i\alpha\tau_3 N_+}{2N}}). \quad (3.25)$$

Once again we have normalized the generator so that the  $S^1$  has length  $2\pi$ . At generic points of the  $r = 0$  subspace, this  $S^1$  does not lie entirely inside the  $T^3$ . However, at

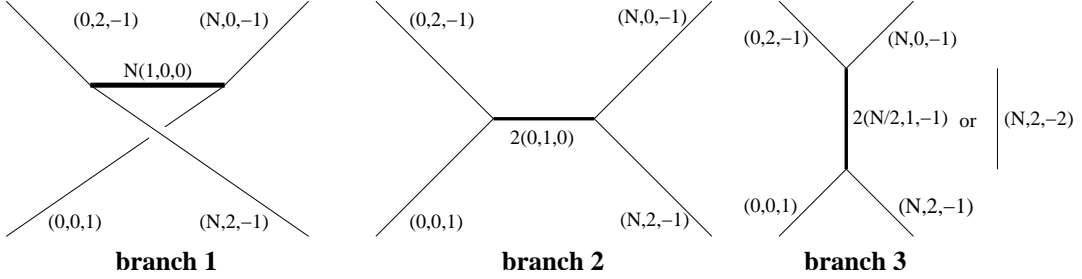


Figure 3: The three branches of  $g = 0$ .

special loci it does. These are as follows:

$$\begin{aligned}
 (N - \frac{N_-}{2}, 1, -1)'' &: (e^{\frac{i\alpha\tau_3}{2}} X e^{\frac{-i\alpha\tau_3 N_+}{2N}}, \tilde{X} e^{\frac{-i\alpha\tau_3 N_+}{2N}}) \leftrightarrow (r = 0, \theta = 0), \\
 (-\frac{N_-}{2}, -1, 1)'' &: (e^{-\frac{i\alpha\tau_3}{2}} X e^{\frac{-i\alpha\tau_3 N_+}{2N}}, \tilde{X} e^{\frac{-i\alpha\tau_3 N_+}{2N}}) \leftrightarrow (r = 0, \theta = \pi), \\
 (-\frac{N_-}{2}, -1, 0)'' &: (X e^{\frac{i\alpha\tau_3 N_-}{2N}}, e^{\frac{-i\alpha\tau_3}{2}} \tilde{X} e^{\frac{i\alpha\tau_3 N_-}{2N}}) \leftrightarrow (r = 0, \tilde{\theta} = 0), \\
 (-\frac{N_-}{2}, 1, 0)'' &: (X e^{\frac{i\alpha\tau_3 N_-}{2N}}, e^{\frac{i\alpha\tau_3}{2}} \tilde{X} e^{\frac{i\alpha\tau_3 N_-}{2N}}) \leftrightarrow (r = 0, \tilde{\theta} = \pi).
 \end{aligned} \tag{3.26}$$

The diagram for these geometries is presented in figure 4. The lengths of the internal legs, marked as  $\lambda N_+$ ,  $\lambda N_-$  on the diagram, give the sizes of three-cycles in the geometry.

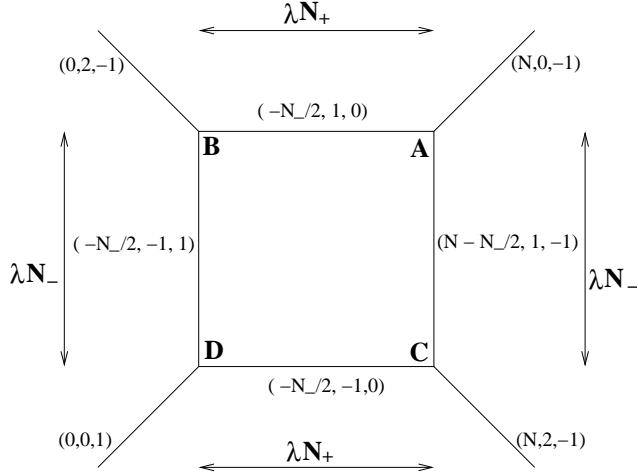


Figure 4: Classical geometries of  $g = 1$ .

It is an interesting exercise to read off various topological properties of  $T^{N_+, N_-}$  from this diagram. For example, the  $T^2$  fibration over internal legs **BA** and **DC** are both lens space  $S^3/\mathbb{Z}_{N_+}$  and are homotopic to each other, and in a similar way the legs **BD** and **AC** both give  $S^3/\mathbb{Z}_{N_-}$ . One can identify them with the lens spaces within  $T^{N_+, N_-}$  defined as submanifolds of fixed  $(\theta, \phi)$  or  $(\tilde{\theta}, \tilde{\phi})$ . One can also read off that the lens spaces  $S^3/\mathbb{Z}_{N_\pm}$  obey one homology relation so that the  $G_2$  geometry has only one parameter. Viewing the graph as a three-dimensional 5-brane web, one can also check that the web is rigid

except for overall rescaling. Later we shall return to this 5-brane web picture to prove that there are no further branches of classical moduli space.

## 4. A dual type IIA picture

We have described several families of  $G_2$  metrics with the same asymptotics and understood the structure of the classical moduli space. We would now like to know how the corresponding quantum moduli space looks. One nice way to study this problem will be to try dimensional reduction along the diagonal  $U(1)$  defined by

$$(g_1, g_2, g_3) \rightarrow (\omega g_1, \omega g_2, \omega g_3), \quad (X, \tilde{X}) \rightarrow (\omega X \omega^{-1}, \omega \tilde{X} \omega^{-1}) \quad (\omega = e^{i\alpha\tau_3})$$

This leads to a dual type IIA picture involving a special lagrangian D6-brane in a non-compact Calabi-Yau manifold which admits a gauged linear sigma model (GLSM) description. The chief advantage of this description is that by moving to the mirror IIB geometry we get an exact description of the quantum moduli space through a certain curve contained in the mirror target space[12].

We begin in this section by translating the classical moduli space obtained in the M-theory analysis to this framework and then study the quantum moduli space within the mirror IIB picture in the following section. The GLSM offers a quantitative description of various blow-ups of the  $\mathbb{Z}_N \times \mathbb{Z}_2$  orbifold in terms of Fayet-Iliopoulos (FI) parameters. The Lagrangian D6-brane is described as a half line in the toric base ending on its boundary. The classical moduli space is therefore described by the FI parameters and the position of the endpoint of the D6-brane. However, as we will explain, some of the FI parameters are effectively frozen due to the presence of the D6-brane.

### 4.1. TORIC DESCRIPTION OF THE ORBIFOLD

The three families of  $\mathbb{Z}_N \times \mathbb{Z}_2$  orbifolds of  $\mathbb{R}^4 \times S^3$  are mapped by the IIA reduction to a Lagrangian D6-brane in the orbifold  $\mathbb{C}^3/(\mathbb{Z}_N \times \mathbb{Z}_2)$

$$(z_1, z_2, z_3) \sim (z_1, e^{\frac{2\pi i}{N}} z_2, e^{-\frac{2\pi i}{N}} z_3) \sim (-z_1, z_2, -z_3). \quad (4.1)$$

The IIA reduction of the  $G_2$  geometries with local  $T^{N+,N-}$  should correspond to a certain blow-up of this orbifold with a D6-brane at a suitable place. Below we will describe these branches of classical moduli space using toric geometry or GLSM.

We first find the toric data for the orbifold  $\mathbb{C}^3/(\mathbb{Z}_N \times \mathbb{Z}_2)$ . Introduce the coordinates  $(z_1, z_2, z_3)$  on  $\mathbb{C}^3$ , and associate to them the basis vectors  $(1, 0, 0), (0, 1, 0), (0, 0, 1)$  of a three-dimensional lattice  $\mathbf{N}$ . In toric geometry, they are the edge vectors and constitute

the toric fan of  $\mathbb{C}^3$  made of a single cone (positive octant of  $\mathbb{R}^3$ ) and  $\mathbf{N}$  is the lattice of  $\mathbb{C}^\times$  actions on  $\mathbb{C}^3$ :

$$(n_1, n_2, n_3) \in \mathbf{N} : (z_1, z_2, z_3) \rightarrow (t^{n_1} z_1, t^{n_2} z_2, t^{n_3} z_3). \quad (4.2)$$

The orbifold is described by the cone generated by the same vectors, but the lattice  $\mathbf{N}'$  of  $\mathbb{C}^\times$  actions is finer due to the orbifolding and is generated by

$$\rho_1 = \frac{1}{2}(1, 0, -1), \quad \rho_2 = \frac{1}{N}(0, 1, -1), \quad \rho_3 = (0, 0, 1).$$

The toric fans are given in the two diagrams on the left of figure 5 in the cases  $N = 5$  and  $N = 4$ .

Let us refer to the triangle spanned by  $(1, 0, 0), (0, 1, 0), (0, 0, 1)$  as  $\Delta$  in what follows. The various toric blow-ups of the orbifold singularity are described by the introduction of new edge vectors and the subdivision of the positive octant into smaller cones. For Calabi-Yau blow-ups, the new edge vectors should be chosen from the lattice points on  $\Delta$  which are depicted by  $\bullet$ 's in the figure. One can include as many new edges as one wishes, but the orbifold singularity is completely resolved when all the possible edges are included. The two figures on the right of figure 5 show examples of maximal blow-ups.

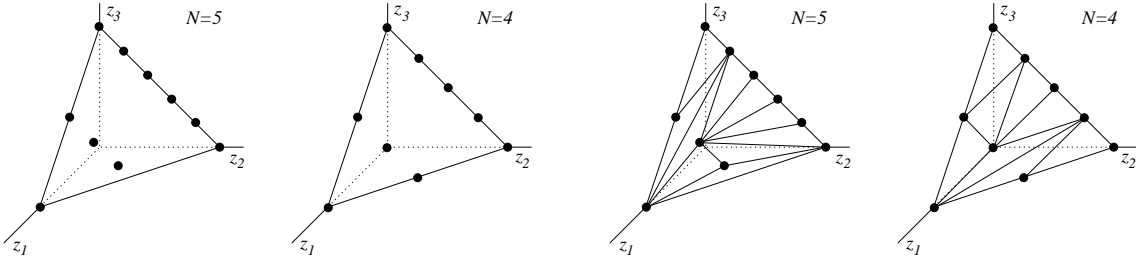


Figure 5: The toric fans for the orbifolds  $\mathbb{C}^3/(\mathbb{Z}_N \times \mathbb{Z}_2)$  and their maximal resolutions.

The blown-up geometries are conveniently described by a GLSM as classical moduli spaces of vacua. The GLSM associates a matter field  $z_i$  to each edge vector  $v_i$ , and a  $U(1)$  gauge symmetry  $U(1)_a : z_i \rightarrow e^{i\alpha Q_i^\alpha} z_i$  to each linear relation among the edges,  $\sum_i Q_i^a v_i = 0$ . For maximal blow-ups there are  $(k+3)$  matter fields and  $k$   $U(1)$ 's with  $k \equiv [\frac{3N}{2}]$ . Different blown-up manifolds are then described by different level sets of D-term conditions

$$\sum_i Q_i^a |z_i|^2 = r_a, \quad (4.3)$$

modulo gauge equivalence. The various subdivisions of the positive octant of the previous paragraph (triangulations of  $\Delta$ ) describe the fact that  $\{z_i, z_j, z_k\}$  can simultaneously vanish if and only if  $\{v_i, v_j, v_k\}$  form a cone. For a suitably chosen basis of  $U(1)$ 's, the manifold

has large blown up cycles when the  $r_a$ 's are large and positive whilst the resolutions are turned off for sufficiently negative  $r_a$ 's.

Regarding toric Calabi-Yau threefolds as  $T^3$  or  $T^2 \times \mathbb{R}$  fibrations, one can draw the toric skeletons [16, 17] or webs [18] which describe where and how the fiber degenerates in the base. These diagrams are convenient for describing the various branches of classical moduli space.

Let us first look at the orbifold with no resolution modes turned on, corresponding to the  $g = 0$  branch. The skeleton is obtained in the following way. Choose as the basis 1-cycles of the  $T^3$  fiber, the three  $U(1)$ 's corresponding to the lattice points  $\rho_{1,2,3}$  and denote them by  $\alpha_{1,2,3}$ . Since

$$(1, 0, 0) = 2\rho_1 + \rho_3, \quad (0, 1, 0) = N\rho_2 + \rho_3, \quad (0, 0, 1) = \rho_3, \quad (4.4)$$

the three  $U(1)$  moment maps  $|z_i|^2$  generate translations along the 1-cycles

$$|z_1|^2 \leftrightarrow 2\alpha_1 + \alpha_3, \quad |z_2|^2 \leftrightarrow N\alpha_2 + \alpha_3, \quad |z_3|^2 \leftrightarrow \alpha_3.$$

The base of the  $T^3$  fibration is identified with the first octant of an  $\mathbb{R}^3$  parametrized by the moment maps  $|z_i|^2$ . The  $T^3$  fibre degenerates to a  $T^2$  at generic points on the boundary where one of the  $z_i$  vanishes, and further to an  $S^1$  on the three coordinate axes. This information is summarized in the skeleton diagram given on the left of figure 6.

On each leg of the skeleton one can find a vanishing cycle of the form  $n_1\alpha_1 + n_2\alpha_2$ . By projecting the skeleton onto a 2-plane so that the leg with vanishing cycle  $n_1\alpha_1 + n_2\alpha_2$  is lying along the vector  $(n_1, n_2)$ , we obtain a web diagram as shown on the right of figure 6.

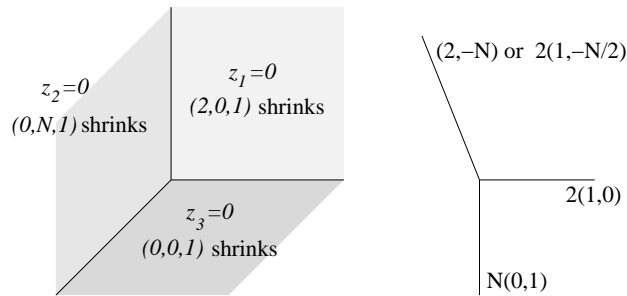


Figure 6: The skeleton and web for the orbifold.

A nice thing about the web is that it can be directly interpreted as the  $(p, q)$  5-brane web in a IIB dual [16]. The  $(p, q)$ -charges of the 5-brane legs and their angles at junction points are simply understood from supersymmetry, charge conservation and balance of the tension.

Let us also present the toric fan, skeleton and web diagrams for a partial blow-up of the orbifold where only one mode corresponding to the edge

$$\left(\frac{1}{2}, \frac{N_-}{2N}, \frac{N_+}{2N}\right) = \rho_1 + \frac{N_-}{2}\rho_2 + \rho_3 \quad (4.5)$$

is turned on. Blow-ups of this form will turn out to describe the  $g = 1$  branches after the D6-brane is added. The GLSM now has four fields  $z_{1,..,4}$  obeying a D-term condition

$$N|z_1|^2 + N_-|z_2|^2 + N_+|z_3|^2 - 2N|z_4|^2 = r.$$

and a  $\mathbb{Z}_N$  orbifold identification  $(z_1, z_2, z_3) \sim (z_1, \omega z_2, \omega^{-1} z_3)$ ,  $\omega^N = 1$ . The orbifold singularity is partially blown up for positive  $r$ . If  $k$  be the greatest common divisor of  $N_+, N_-$  and  $(N, N_+, N_-) = k(n, n_+, n_-)$ , then the resolved target space is a  $\mathbb{Z}_k$  orbifold of the canonical bundle over a weighted projective space  $\mathbb{WP}_{n, n_+, n_-}^2$ . The coordinates  $z_{1,2,3}$  cannot vanish simultaneously so the tip of the positive octant is chopped off from the base of  $T^3$  fibration. See figure 7 below.

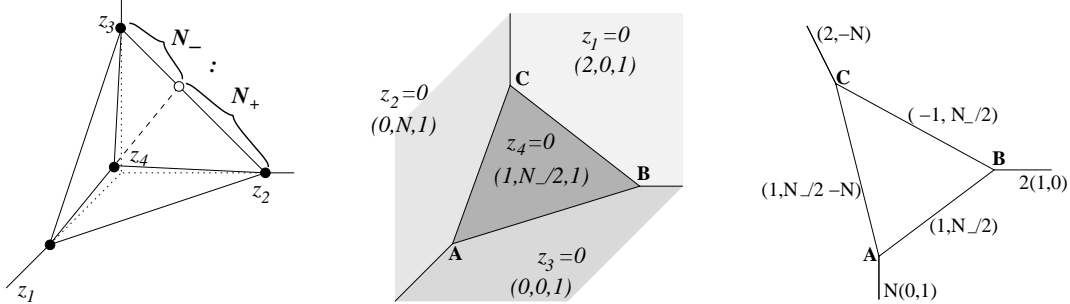


Figure 7: A partial resolution of the orbifold singularity.

Similarly, turning on modes corresponding to vectors sitting on the edges of the triangle  $\Delta$  (i.e., lattice points on the boundary of  $\Delta$  excluding the three vertices) will chop off the base of the  $T^3$  fibration along the coordinate axes, and in particular will increase the number of semi-infinite legs in the skeleton or web diagrams. These are all resolutions of a line of  $\mathbb{C}^2/\mathbb{Z}_N$  or  $\mathbb{C}^2/\mathbb{Z}_2$  orbifold singularities. Although non-normalizable, one is free to turn on these modes to deform the theory in the absence of the Lagrangian D6-brane. After adding the D6-brane the situation changes drastically as we shall explain later.

For even  $N$ , one can also deform the orbifold singularity so that the web consists of two disjoint parts, each of which is made of three legs with charges  $(1, 0)$ ,  $(0, N/2)$  and  $(-1, N/2)$  as in figure 8. The deformation creates a 3-cycle of topology  $S^2 \times S^1$ , corresponding to a vertical line segment stretching between parallel 5-brane legs.

## 4.2. LAGRANGIAN D6-BRANES

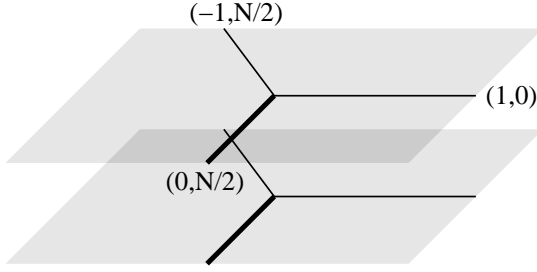


Figure 8: A deformation for even  $N$ .

Lagrangian D6-branes of topology  $\mathbb{C} \times S^1$  are described by half-lines in the toric base ending on a leg of the skeleton [17, 19]. In the GLSM description of a toric CY involving with  $k+3$  coordinates,  $z_i$ , obeying  $k$  D-term equations and a  $U(1)^k$  equivalence relation, the relevant branes have one direction along the toric base and two along the fiber. They are therefore defined by two further linear constraints on  $|z_i|^2$  and one linear constraint on  $\arg(z_i)$ . The constraint on  $\arg(z_i)$  has to be

$$\sum_i \arg z_i = \text{const}$$

for the submanifold to be *special*, and it follows that the  $k+2$  constraints on  $|z_i|^2$  are all of the form

$$\sum_i q_i |z_i|^2 = \text{const}, \quad \left( \sum_i q_i = 0 \right).$$

The solution to the constraints in the base is:  $|z_i|^2 = \xi + c_i$ , ( $\xi \in \mathbb{R}_{\geq 0}$ ). The topology of the brane requires two of the  $|z_i|^2$  vanish at  $\xi = 0$ , which means that the D6-brane must end on a leg of the skeleton.

Classical configurations are therefore described by a half-line ending on a toric skeleton. The three  $g = 0$  branches are described by a D6-brane ending on one of the three legs of the skeleton in figure 6, and the complex modulus corresponds to the position of the endpoint and a  $U(1)$  Wilson line on the brane. For  $g = 1$  branches, we claim that the D6-brane has to end at a certain point on the leg **BC** of the skeleton in figure 7, and the only parameter is the overall scale of the graph. We will verify this by moving to the web picture.

In the web diagram, D6-branes are described as half lines ending on one of the legs and extending orthogonally to the web. However, after moving to the 5-brane web picture in type IIB they turn into TN5-branes carrying KK monopole charges along an  $S^1$  of the target space[12] and bend the web, to produce three-dimensional web of  $(p, q, r)$  5-branes. The three-dimensional web of 5-branes derived in this way should agree with the one obtained in the previous section by  $T^3$  reduction of the M-theory solutions.

Let us start with the geometries with  $g = 0$  described by the two-dimensional 5-brane web with three legs

$$N(0, 1), \quad 2(1, 0), \quad (2, -N)$$

Let us then add a TN5-brane to make the web three-dimensional with four semi-infinite legs. The new external leg has charge  $(0, 0, 1)$ , and the other legs also acquire TN5-brane charges in order to satisfy the charge conservation at junction points. These charges are determined from the following two requirements. First, each external leg should be made of a single brane and not of several coincident branes, since our M-theory solutions did not have any orbifold fixed loci extending toward infinity. Secondly, when the four legs are connected together by one finite leg, the following gauge symmetries should be realized on the internal leg:

$$1 : SU(N), \quad 2 : SU(2), \quad 3 : SU(2) \text{ or none } (N \text{ even or odd})$$

One then finds that, up to redefinition of basis, the four legs must have the charge vectors

$$(0, N, -1), \quad (2, 0, 1), \quad (2, -N, 1), \quad (0, 0, 1) \quad (4.6)$$

This agrees with the result of  $T^3$  reduction shown in figure 3, up to trivial signs and permutations.

Next we consider the  $g = 1$  branches labelled by  $(N_+, N_-)$  and described by the two-dimensional web of figure 7. We first fix the charges of the four external legs as in (4.6) and then try to find the charges of the internal legs and the endpoint of the fourth leg. We obtain in this way the same web as was drawn in figure 4, and furthermore find that the endpoint of the fourth leg should be at a point **D** on the leg **BC** of figure 7 satisfying  $\mathbf{BD} : \mathbf{DC} = N_- : N_+$ . This is necessary in order for the loop inside the web to close once we require that the legs lie in directions imposed by supersymmetry, and it nicely agrees with results from the M-theory geometry and the earlier IIA flux superpotential analysis.

Note that the blow-up modes corresponding to the edges on the faces of  $\Delta$  have disappeared, or have been effectively frozen after introducing the D6-brane, since no external 5-brane legs are made of coincident 5-branes. To recover and turn on those modes, one first has to send the D6-branes off to infinity in an appropriate manner and change the charge of the semi-infinite leg – otherwise the supersymmetry will be broken. Therefore, the theories with non-zero such blow-up modes are infinitely far away from the theories of our interest.

### 4.3. A NO-GO RESULT FOR $g \geq 2$ BRANCHES

We have identified the backgrounds with  $g = 0, 1$  with 5-brane webs of the same *genus*. This is not a coincidence, as the mirror IIB geometry turns out to contain a Riemann surface of the same genus and the genus is indeed related to the number of  $U(1)$  gauge symmetries in the IIB setup.

It is worthwhile to look for possible web configurations of higher genus. This should be considerably easier than finding new  $G_2$  holonomy solutions with the required asymptotics. In fact, we would like to prove the absence of such webs of higher genus.

Balancing tensions in the web requires that the  $(p, q, r)$  charges of the legs add up to zero at each junction point. In this sense the  $(p, q, r)$  are better regarded as currents. Supersymmetry requires that each leg of the web has to lie along a direction determined by its charge vector. Namely, a leg with  $(p, q, r)$  5-brane charge has to extend along the  $(p, q, r)$  direction. Let us introduce a height function on the vertices of the web which gives the position in the  $(0, 0, 1)$  direction. We choose our convention so that  $r$ -current always flows downhill.

From our previous discussion we may restrict attention to webs which have four legs with charges given by (4.6), and which admit a projection to a two-dimensional web corresponding to a blow-up of the orbifold  $\mathbb{C}^3/(\mathbb{Z}_N \times \mathbb{Z}_2)$ . We can therefore only turn on blow-up modes corresponding to edges in the interior of  $\Delta$ , and the genus is at most  $[\frac{N-1}{2}]$ . A two-dimensional web of maximal genus  $g$  is shown in figure 9. The body of the web has the structure of a large triangle partitioned by parallel finite legs of  $(p, q) = (0, 1)$ . What we would like to prove therefore is the following

**No-go result:** *there is no supersymmetric 5-brane web of genus  $\geq 2$  with four external legs of charges (4.6) which admits a projection to a two-dimensional web of the type drawn in figure 9.*

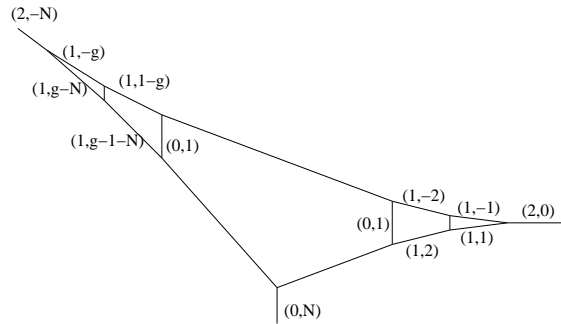


Figure 9: the two-dimensional web for maximal blow-up

In the following we will denote by **A**, **B**, **C**, **D** the vertices where the four external legs of charges  $(0, N, -1)$ ,  $(-2, 0, -1)$ ,  $(2, -N, 1)$ ,  $(0, 0, 1)$  are attached to the body of the web<sup>2</sup>. There are five possible ways of attaching **D** to the web as shown in figure 10.

<sup>2</sup>We have reversed the sign of the  $(-2, 0, -1)$  charge vector relative to our previous convention. This is

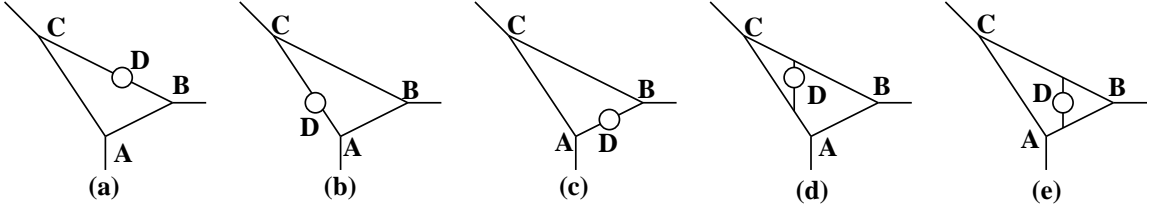


Figure 10: the five choices for the location of the  $(0, 0, 1)$  5-brane.

The external legs at **A** and **B** are sources of a unit  $r$ -current whilst the legs at **C** and **D** are sinks. The height function is therefore not constant on the the web. We begin by trying to identify the lowest and highest vertices.

Since  $r$ -current flows downhill, there can be no current flowing out of the lowest vertex. Thus the lowest vertex must either be one of the sinks **C**, **D** or else a vertex at which there is no flow of current in or out. In the latter case, all neighbouring vertices will also be lowest vertices and this will continue along any path until we hit **C** or **D**.

A brief inspection of figures 9 and 10 shows that every internal vertex on the web can be connected either to **A** or to **B** by a path which avoids **C** and **D**. Thus if any internal vertex is lowest then, by following the path, we would find that **A** or **B** is also a lowest vertex which is a contradiction since they are sources for current. We can conclude that **C** and **D** are the lowest vertices and also that they are neighbours with no junction points in between.

By a similar reasoning, **A** and **B** are the highest vertices and are also neighbours. These requirements prohibit webs of types (c),(d),(e) in figure 10. The only allowed webs are those of type (a) or (b) with no junction points on **AB** and **CD**.

Now let us make a basis change of the charge vectors  $(p, q, r) = (p, q, r - p)'$ . This will change the labels of external legs as

$$\mathbf{A}(0, N, -1)', \quad \mathbf{B}(-2, 0, 1)', \quad \mathbf{C}(2, N, -1)', \quad \mathbf{D}(0, 0, 1)'$$

and in particular the role of **B**, **C** as a source and a sink of  $r$ -current are exchanged. This redefinition of charges transforms the webs (b) and (c) of figure 10 into each other, so if one is inconsistent so is the other. Applying this redifinition to the web (a) one finds that the paths of highest and lowest points are now given by **AC** and **BD**. There should be no junction points on these legs as well as **AB** and **CD**, so the internal legs of  $(p, q) = (0, 1)$  cannot end anywhere. We have shown that the only consistent webs are of type (a) with no additional legs. They are precisely the  $g = 1$  configurations discussed in the previous subsection.

---

so that the total charge flowing into the diagram is vanishing. For the present argument we need to be careful of such sign choices.

## 5. IIB mirror

Now we turn to the analysis of the quantum moduli space. We would like to obtain its holomorphic structure by working in the mirror type IIB picture. The target space is given by a hypersurface in  $\mathbb{C}^4$ :

$$\xi\eta = F(u, v; t_i), \quad (5.1)$$

where  $t_i$  parametrizes the complex structure. The curve  $\Sigma : F(u, v; t_i) = 0$  has the same topology as the toric skeleton of the previous section with the legs “fattened”. The lagrangian D6-brane turns into a D5-brane at  $\xi = 0$  extending along  $\eta$ -direction and intersecting with the curve  $\Sigma$  at a point  $(u_0, v_0)$ . The superpotential as a function of  $(u, t_i)$  is given by[17, 19]

$$W(u, t_i) = \int_{u^*}^{u_0} v(u; t_i) du. \quad (5.2)$$

with a suitably chosen reference point  $(u^*, v^*)$ . In the following, we will first derive the curve  $\Sigma$  starting from the GLSM of the previous section, clarifying in particular the relation between  $t_i$  and the complexified Kähler moduli on the IIA side. We will then give a precise form of the superpotential and the F-term equations for our system. Finally the exact holomorphic structure of the quantum moduli space will be obtained for some examples with small  $N$ .

For mathematical background on complex curves, we refer the reader to [20].

### 5.1. CURVE WITHIN THE MIRROR GEOMETRY

Let us first derive the curve  $\Sigma$  for our  $\mathbb{Z}_N \times \mathbb{Z}_2$  orbifold of  $\mathbb{C}^3$ . We should start with the linear sigma model in the IIA side with all the blow-up modes taken into account. There are therefore  $k + 3$  chiral matter fields  $z_i$  obeying  $U(1)^k$  equivalence relations and  $k$  D-term conditions, with  $k = [3N/2]$ . Let us regard  $z_{1,2,3}$  as the original coordinates of  $\mathbb{C}^3/(\mathbb{Z}_N \times \mathbb{Z}_2)$  and the rest as corresponding to blow-ups, and choose the set of FI parameters  $r_a$  so that the D-term conditions take the form

$$\sum_{i=1,2,3} Q_i^a |z_i|^2 + \sum_{b=1}^k Q_{3+b}^a (|z_{3+b}|^2 + r_b) = 0. \quad (5.3)$$

We will refer to  $r_b$  as the blow-up mode corresponding to the edge vector for  $z_{3+b}$ . The mode is turned on or off when  $r_b$  is large positive or negative. Indeed, when  $r_b$  is large negative the field  $z_{3+b}$  has to condense and become massive along with one of the  $U(1)$ ’s, so they disappear from the low-energy physics.

Mirror symmetry [21] transforms these matter fields into  $k + 3$  twisted chiral fields  $Y_i$  related by  $\text{Re}Y_i = |z_i|^2$ , and maps the GLSM to a Landau-Ginzburg model. These twisted

matter fields obey  $k$  linear relations that follow from the D-term conditions. They are solved in terms of three fields  $u, v, w$  as

$$Y_i = a_i u + b_i v + c_i w - t_i; \quad \begin{pmatrix} t_{1,2,3} = 0, \\ t_{3+b} = r_b + i\theta_b \quad (b = 1, \dots, k) \end{pmatrix}$$

where  $(a_i, b_i, c_i)$  is the edge vector  $v_i = a_i \rho_1 + b_i \rho_2 + c_i \rho_3$  corresponding to  $z_i$ , and  $r_b + i\theta_b$  are complexified Kähler parameters. The LG model of  $\{u, v, w\}$  has the superpotential  $W_{\text{LG}} = \sum_i e^{-Y_i}$ . Since  $c_i = 1$  for all the edge vectors of our toric fan under the choice of lattice basis (4.4), the dependence of  $W_{\text{LG}}$  on  $w$  factorizes:

$$W_{\text{LG}} = e^{-w} \sum_i e^{-a_i u - b_i v + t_i} = e^{-w} F(u, v; t_i).$$

As explained in [22], this LG model is equivalent to the sigma model on a CY space (5.1).

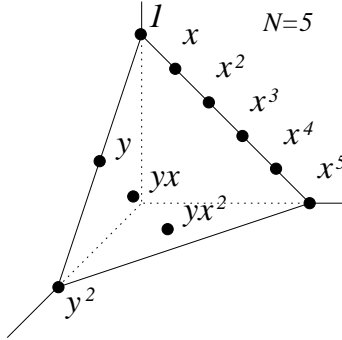


Figure 11: Monomials of  $x, y$  corresponding to edges of the fan.

Introducing  $e^{-u} = y, e^{-v} = x$  one finds that each edge vector is associated to a monomial  $y^{a_i} x^{b_i}$  in  $F$  as in figure 11. The curve  $\Sigma$  is expressed in terms of  $x, y$  as

$$F(x, y; t_i) = y^2 - 2yP(x; t_i) + Q(x; t_i) = 0. \quad (5.4)$$

where  $P$  and  $Q$  are polynomials of  $x$  of degree  $[\frac{N}{2}]$  and  $N$  respectively, and the coefficient of each monomial is given in terms of the corresponding Kähler parameter as  $e^{t_i}$ . The curve therefore has genus  $[\frac{N-1}{2}]$  for generic values of the Kähler parameters.

Looking at the toric fan, there are as many edge vectors in the interior of  $\Delta$  as the genus  $g$  of  $\Sigma$ . These correspond to normalizable deformations of the target space. Indeed, for each 1-cycle  $\alpha$  of the curve  $\Sigma$  there corresponds a 3-cycle defined by a circle fibration over a 2-disc bounded by  $\alpha$ , with the fiber being the nontrivial  $S^1$  of the cylinder  $\xi\eta = F(x, y)$  in  $\xi\eta$  space. One can count normalizable deformations of complex structure by counting mutually non-intersecting compact 3-cycles, and there are  $g$  of them. Also, there arise  $g$   $U(1)$  gauge fields from dimensional reduction of the IIB 4-form potential along the dual 3-cocycles.

On the other hand, the edge vectors sitting on the faces of  $\Delta$  correspond to non-normalizable deformations as they alter the asymptotic form of the curve. Recall that the variables  $x, y$  are defined from the LG fields, so that they are  $\mathbb{C}^\times$ -valued. The curve  $\Sigma$  written in terms of  $x, y$  therefore has several punctures. The coefficients of monomials on the face of figure 11 connecting  $(0, 1, 0)$  and  $(0, 0, 1)$  determine the location of the punctures at  $y = 0$ , and similarly for the other two faces. They are also related to the separation of the parallel semi-infinite legs of the skeleton or web in the IIA picture. As such, they are clearly non-normalizable.

Depending on whether  $N$  is even or odd, the curve has  $(N + 2 + 2)$  or  $(N + 2 + 1)$  punctures for generic choices of the non-normalizable complex structure parameters. The curve of interest to us should have only three punctures, so we fix some of the coefficients in the definition of curve by requiring that[12]

1.  $F(x, 0)$  has a degenerate root of order  $N$ ,
2.  $F(0, y)$  has a double root,
3.  $\hat{F}(y) \equiv \lim_{x \rightarrow \infty} x^{-N} F(x, yx^{N/2})$  has a double root when  $N$  is even.

(5.5)

One can rescale  $x, y$  so that the first two punctures are at  $(x, y) = (1, 0)$  and  $(0, 1)$ . The curve should thus take the form

$$0 = F(x, y) = y^2 + (1 - x)^N - 2yP(x; s_i) \quad (5.6)$$

with

$$\begin{aligned} (N = 2n) \quad P(x; s_i) &= 1 + s_1x + \cdots + s_nx^n, \quad s_n \equiv \pm 1 \\ (N = 2n + 1) \quad P(x; s_i) &= 1 + s_1x + \cdots + s_nx^n \end{aligned} \quad (5.7)$$

We are left with normalizable deformations corresponding to the interior points of  $\Delta$ . In the following we denote by **A**, **B**, **C** the three punctures at  $(x, y) = (1, 0), (0, 1), (\infty, \infty)$ .

Note that, with no D5-branes and  $\mathcal{N} = 2$  spacetime supersymmetry, there is nothing wrong with considering the whole family of theories related by non-normalizable deformations. This situation changes drastically when the D5-brane is added and a superpotential (5.2) is generated. Furthermore, we will see that many of the normalizable deformations are fixed and the curve cannot have genus  $\geq 2$  owing to the presence of the superpotential.

## 5.2. SUPERPOTENTIAL

Now we turn to the analysis of the superpotential (5.2) generated by the D5-brane. The integral contains an undetermined reference point  $(u^*, v^*)$ , so that  $W$  has an ambiguity up to a (possibly  $t_i$ -dependent) constant shift. We will first fix this ambiguity by the following simple argument.

Recall that in the previous section we obtained a description of the moduli space in terms of three-dimensional webs with four external legs

$$(0, N, -1), (2, 0, 1), (2, -N, 1), (0, 0, 1).$$

Starting from a two-dimensional web with external legs  $(0, N), (2, 0), (2, -N)$ , one can reproduce the above set of legs as illustrated in figure 12. We put two  $(0, 0, 1)$  5-brane lines anywhere on the web. Once they intersect with the legs of the web each of them breaks into halves. One sends three of the four half-lines to infinity along the external legs of the original web to alter their charges, thereby arriving at the three-dimensional web with the required external legs.

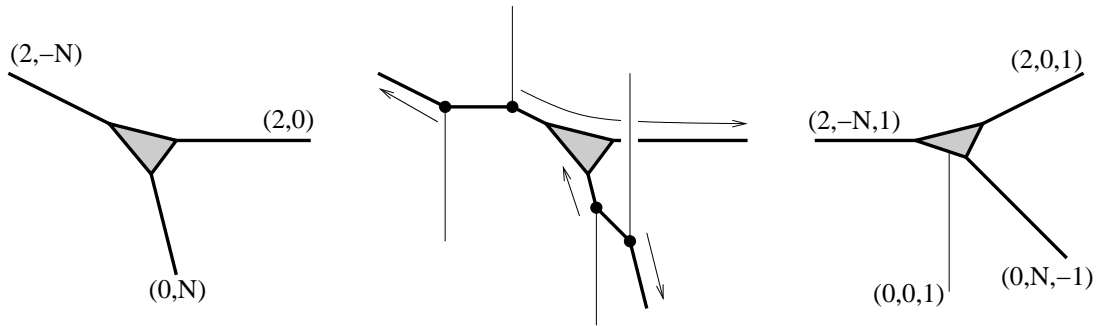


Figure 12: Construction of three-dimensional webs from two-dimensional ones.

The interpretation of this procedure in the mirror IIB side is clear. A D5-brane with worldvolume  $\xi\eta = F(u, v) = c$  decomposes into a D5-brane with  $\xi = 0$  and a  $\bar{D}5$ -brane with  $\eta = 0$  when it touches the curve, i.e. when  $c$  vanishes. We should therefore attach two pairs of D5,  $\bar{D}5$ -branes to the curve, and bring  $\bar{D}5$ -branes to the punctures **A**, **B** and a D5-brane to **C**. We will refer to the remaining free D5-brane as **D**. The superpotential is then given by an integral of the form (5.2) over the contour produced by the pairs of D5-branes,

$$W = \int_{\mathbf{B}}^{\mathbf{C}} v du + \int_{\mathbf{A}}^{\mathbf{D}} v du. \quad (5.8)$$

Several comments are in order. First, for curves with genus  $g \geq 1$ , the integration contour is still ambiguous due to the presence of non-trivial one-cycles. This ambiguity is related to the fact that, by moving a D5-brane along a closed contour on the curve, one can induce a RR3-form flux. So topologically different contours lead to different flux backgrounds. One could also try writing the superpotential as

$$W = \int_{\mathbf{B}}^{\mathbf{D}} v du + \int_{\mathbf{A}}^{\mathbf{C}} v du.$$

This leads to the same superpotential as long as the difference between the two contours is trivial;

$$(\mathbf{BC} + \mathbf{AD}) - (\mathbf{BD} + \mathbf{AC}) = \mathbf{AD} + \mathbf{DB} + \mathbf{BC} + \mathbf{CA} = 0 \in H_1(\Sigma)$$

We will present the solution to the F-term equations  $\partial_{s_j} W = 0$  in a way that avoids complications due to this ambiguity and the contour will be denoted simply as  $\int_{\overline{\text{D5}}}^{\text{D5}}$ .

The second comment concerns the parameters of the theory. Moving the free D5-brane  $\mathbf{D}$  is clearly a non-normalizable deformation and in that sense would appear to be on an equal footing with the deformations of the curve that change the positions of punctures. However, as labels of theories one should not regard these two kinds of parameters on the same footing. This is because the superpotential (5.8) is not well-defined without regularizing the divergence of the integral near each end of the contour at the punctures. While the regulator is independent of the position of  $\mathbf{D}$ , it should depend on the position and multiplicity of punctures. As a result, the variation of  $W$  under the motion of  $\mathbf{D}$  still makes sense but the variation under the non-normalizable deformation of the background does not. Since we want the theories in a given family to be defined by the same regularization, the position of  $\mathbf{D}$  is the only relevant parameter of the theory<sup>3</sup>.

Our superpotential has a further ambiguity up to  $SL(2, \mathbb{Z})$  linear transformations of  $u, v$ . Such a subtlety was discussed in detail in [17, 19, 12]. There it was shown that, under a suitable choice of coordinates, the mirror IIB superpotential for a simpler orbifold  $(\mathbb{C}^2/\mathbb{Z}_N) \times \mathbb{C}$  exactly reproduces the topological A-model amplitude for the relevant large  $N$  transition of the conifold. We will not need to go into the details of this ambiguity, since in our case it only shifts  $W$  by some constants independent of  $s_i$ , and we will only consider the variations of  $W$  with respect to the  $s_i$ .

Let us turn to the analysis of supersymmetric vacua of the theory. We introduce new coordinates  $x, \hat{y}$  to rewrite the curve as

$$\Sigma : y^2 - 2yP(x; s_i) + (1-x)^N = \hat{y}^2 + (1-x)^N - P(x; s_i)^2 = 0 \quad (5.9)$$

The curve is then a standard double cover of the  $x$ -plane with  $2g + 2$  branching points (including  $x = \infty$ ). The superpotential and its moduli-derivatives now read,

$$W = \int_{\overline{\text{D5}}}^{\text{D5}} \frac{\log y dx}{x} , \quad \frac{\partial W}{\partial s_j} = \int_{\overline{\text{D5}}}^{\text{D5}} \frac{x^{j-1} dx}{\hat{y}} \quad (j = 1, \dots, g = [\frac{N-1}{2}]). \quad (5.10)$$

The  $s_j$ -derivatives of  $vdu$  give the set of  $g$  independent holomorphic 1-forms on  $\Sigma$ .

In mathematical terms, the formal difference between the set of D5-branes and  $\overline{\text{D5}}$ -branes defines a divisor  $D$  of  $\Sigma$ . Its is of degree zero, i.e., the number of D5-branes is the

---

<sup>3</sup>It may be helpful to recall that the difference between the two types of parameters is particularly clear in the 5-brane web picture of the moduli space, where after the addition of the  $TN$  5-brane charge, the external legs of the web can no longer be separated.

same as the number of  $\overline{\text{D}5}$ -branes. The F-term equations define a map  $\mu$  from divisors of degree zero to the Jacobian variety of  $\Sigma$

$$J_g(\Sigma) = \mathbb{C}^g / \Lambda,$$

where  $\Lambda$  is the period lattice representing the ambiguity in the choice of contours. The F-term conditions require  $\mu(D) = 0 \in J_g(\Sigma)$ , namely that the  $g$  period integrals vanish under a suitable choice of contours connecting D5-branes and  $\overline{\text{D}5}$ -branes.

By Abel's theorem,  $\mu(D)$  vanishes modulo periods if and only if there is a meromorphic function on  $\Sigma$  with poles precisely at D5-branes and zeroes at  $\overline{\text{D}5}$ -branes. Therefore, in our problem the F-term condition is solved by choosing the moduli  $s_i$  for which there exists a meromorphic function on  $\Sigma$  with poles at **C**, **D** and zeroes at **A**, **B**. Such a function, if it exists, defines a map from  $\Sigma$  to  $\mathbb{P}^1$  of degree two. It is known that on hyperelliptic curves there are always such degree two maps  $\Sigma \rightarrow \mathbb{P}^1$ , but it is also known that all such maps are related to the map  $x$  by fractional linear transformation. Since **A**, **B**, **C** are located at points with different values of  $x$ , we conclude that hyperelliptic curves ( $g \geq 2$ ) cannot solve the F-term conditions. This is in perfect agreement with the no-go result for webs of genus  $\geq 2$  which we found earlier!

From the above argument it appears to follow that for  $N \geq 5$  there is no solution to the F-term condition, but this is not the case. The important point is that the curve can have a smaller genus for special choices of moduli due to degeneration of branch points. For such degenerate curves of genus  $g' \leq g$ , one can consider reduced maps  $\mu' : \text{Div}^0(\Sigma) \rightarrow J_{g'}(\Sigma)$ . For  $g' = 1$  we expect a solution to  $\mu'(D) = 0$  modulo periods. Of course, for  $g' = 0$  the condition  $\mu'(D) = 0$  is vacuous.

What about the remaining  $(g - g')$  conditions? To solve these, one must recall that the drop in genus comes from a degeneration of cycles in  $\Sigma$ . This is accompanied by the emergence of massless monopole hypermultiplets associated to D3-branes wrapping the corresponding shrinking 3-cycles of the CY. Let us be schematic here and parametrize the moduli space of  $\Sigma$  by  $(t_1, \dots, t_g)$ , and suppose that a monopole  $M_i, \tilde{M}_i$  becomes light near the locus  $t_i = 0$  ( $i = 1, \dots, g - g'$ ). The superpotential near such a locus is modified by terms containing monopole fields,

$$W(t) \longrightarrow W(t) + \sum_{i=1}^{g-g'} t_i M_i \tilde{M}_i. \quad (5.11)$$

The variation with respect to  $M_i, \tilde{M}_i$  require  $t_i = 0$ , namely that the curve is of reduced genus. Moreover, the  $(g - g')$  remaining conditions corresponding to the vanishing of the  $t_i$ -variations, merely determine the values of the monopole condensates.

We thus arrived at a rough understanding of the structure of the quantum moduli space. We regard the position of the free D5-brane **D** on  $\Sigma$  as the coordinate on moduli

space. For each choice of the position of  $\mathbf{D}$  there will be a certain number of solutions to the F-term condition, which are curves of genus 0 or 1. The  $g = 1$  branches can meet with  $g = 0$  branches at points of monopole condensation.

### 5.3. RESOLUTION OF SINGULARITIES

The light monopoles are identified with D3-branes wrapped on certain compact 3-cycles in the target space. Each such 3-cycles is defined as a circle fibration over a 2-disc bounded by the non-trivial 1-cycle  $\alpha$  of  $\Sigma$ , so it shrinks precisely when  $\alpha$  shrinks. The target space then develops a conifold singularity, since near the degenerate branch point of  $\Sigma$  at  $x = x_0$  the target space is locally described by

$$\xi\eta - \hat{y}^2 + c(x - x_0)^2 + \mathcal{O}((x - x_0)^3) = 0.$$

The condensation of D3-branes blows up the singularity as discussed in [23, 24]. The double-point singularity of the curve is also resolved into two distinct points on the blown-up  $\mathbb{P}^1$ . The 1-cycle  $\beta$  which had non-zero intersection number with  $\alpha$  is pinched off, and we end up with a smooth curve of lower genus in a blown-up target space.

One has to require that the degeneration of branch points of the curve should not occur at the points **A**, **B**, **C**, because this would change the asymptotics of the curve. We will call curves with degenerate branch points at punctures *singular*. A curve is singular when one of the following conditions is satisfied (the third possibility is only for even  $N$ ):

$$P(1) = 0, \quad 2s_1 + N = 0, \quad 2s_{\frac{N}{2}-1} + Ns_{\frac{N}{2}} = 0. \quad (5.12)$$

Singular curves have singularities of the generalized conifold type,  $\xi\eta - \hat{y}^2 + \hat{x}^n = 0$  with  $n \geq 2$  at one of **A**, **B**, **C**. An exception is the case with  $N$  even and  $P(x) = (1 - x)^{N/2}$  for which the target space becomes an  $A_1$  singularity fibered over the  $x$ -plane,  $\xi\eta - \hat{y}^2 = 0$ .

### 5.4. RELATION TO M-THEORY CURVE

Curves of genus zero describe the moduli space of vacua with trivial Wilson lines and no low energy  $U(1)$  gauge symmetry. The D5-brane  $\mathbf{D}$  can move on this curve freely and so its position on the curve serves as a good coordinate on this branch of moduli space. In other words, the  $g = 0$  branch of moduli space is identified with the  $g = 0$  curve. Here we would like to relate these  $g = 0$  curves with the moduli spaces obtained earlier from M-theory.

We first relate the functions  $\eta_{1,2,3}$  on the  $g = 0$  branch found in the M-theory analysis to various disc instanton factors of the type IIA GLSM picture, and then to coordinates  $x, y$  of the IIB picture. The three classical  $g = 0$  phases were described in IIA by a D6-brane ending on one of the three legs of the toric skeleton.

Phase 1 corresponds to the D6-brane ending at  $|z_1|^2 = c, z_2 = z_3 = 0$ , and similarly for the other phases. In these three phases the disc instantons take the form

$$(1) : \{|z_1|^2 \leq c\}/\mathbb{Z}_2, \quad (2) : \{|z_2|^2 \leq c\}/\mathbb{Z}_N, \quad (3) : \begin{cases} \{|z_3|^2 \leq c\}/\mathbb{Z}_N & (N \text{ even}), \\ \{|z_3|^2 \leq c\}/\mathbb{Z}_{2N} & (N \text{ odd}). \end{cases} \quad (5.13)$$

They are related to the lens spaces  $Q'_{1,2,3}$  of (3.3) upon lifting back to M-theory. Using the correspondence between GLSM and LG coordinates  $Y_i \leftrightarrow |z_i|^2$  we find  $y \sim V(Q'_1)$  around the large volume point 1 on the quantum moduli space, and  $x \sim V(Q'_2)$  around the point 2. By comparing with the table 1 we find

$$\eta_1 = x, \quad \eta_2 = y^{-1}, \quad \eta_3 = \begin{cases} s_{N/2} \cdot yx^{-N/2} & (N \text{ even}) \\ y^2 x^{-N} & (N \text{ odd}). \end{cases} \quad (5.14)$$

The coefficient  $s_{N/2}$  in the expression for  $\eta_3$  is necessary so that  $\eta_3 = 1$  at the point 3.

One can translate the parametric representation (3.4) of the M-theory curve for  $g = 0$  to type IIB variables using the relations above, and one obtains a curve of the form (5.6) with

$$P(x) = \frac{1}{2} \left\{ (1 + x^{1/2})^N + (1 - x^{1/2})^N \right\} = \sum_{j=0}^{[N/2]} \frac{N! x^j}{(2j)!(N-2j)!}. \quad (5.15)$$

For even  $N$  the fermion anomaly argument requires  $s_{N/2} = +1$ .

Our analysis of the asymptotics showed that there are two families of curves labeled by  $s_{N/2} = \pm 1$  when  $N$  is even. The moduli space of vacua may consist of several  $g = 1$  branches some of which are with  $s_{N/2} = 1$  and the other are with  $s_{N/2} = -1$ , but only those with  $s_{N/2} = 1$  can be connected to the  $g = 0$  branch. It would be interesting to find out what the label  $s_{N/2}$  corresponds to in the previous pictures.

## 5.5. BRANCH STRUCTURE

The defining equation for curves of reduced genus  $g$  should look like

$$\begin{aligned} (N = 2n) \quad \hat{y}^2 &= P_n(x)^2 - (1 - x)^N = G_{2g+1}(x)H_{n-g-1}(x)^2, \\ (N = 2n + 1) \quad \hat{y}^2 &= P_n(x)^2 - (1 - x)^N = G_{2g+1}(x)H_{n-g}(x)^2, \end{aligned} \quad (5.16)$$

where  $P(0) = 1$ . Here and in the following we put degrees of polynomials as the suffix. The highest coefficient of  $P(x)$  has to be  $\pm 1$  when  $N$  is even, but it is automatic from the above ansatz. We will refer to the curve with double roots removed,  $\tilde{y}^2 = G_{2g+1}(x)$ , as the *reduced curve*.

We have seen that the reduced curves of  $g = 0$  satisfy the F-term conditions no matter where **D** is, as its location is just related to the values of monopole condensates. So the  $g = 0$  branch of the moduli space is the  $g = 0$  curve itself (not the reduced curve). On the

other hand, on  $g = 1$  branches the complex structure of  $\Sigma$  is determined by the position of  $\mathbf{D}$  so that there exists a meromorphic function with poles at  $\mathbf{A}, \mathbf{B}$  and zeroes at  $\mathbf{C}, \mathbf{D}$ . The location of  $\mathbf{D}$  and the moduli of a genus one curve are related in the following way. Suppose  $\mathbf{C}$  is at  $(x, \tilde{y}) = (\infty, \infty)$  on the reduced curve  $\tilde{y}^2 = G_3(x)$ . Then one can define a map from the reduced curve to its Jacobian variety

$$\mu_{\mathbf{C}}(\mathbf{X}) = \int_{\mathbf{C}}^{\mathbf{X}} \frac{dx}{\tilde{y}},$$

in terms of which the F-term condition can be expressed as

$$\mu_{\mathbf{C}}(\mathbf{D}) = \mu_{\mathbf{C}}(\mathbf{A}) + \mu_{\mathbf{C}}(\mathbf{B}).$$

The condition for this to hold is

$$\begin{vmatrix} 1 & x_{\mathbf{A}} & \tilde{y}_{\mathbf{A}} \\ 1 & x_{\mathbf{B}} & \tilde{y}_{\mathbf{B}} \\ 1 & x_{\mathbf{D}} & -\tilde{y}_{\mathbf{D}} \end{vmatrix} = 0. \quad (5.17)$$

On the  $g = 1$  branches we shall use the notation  $(x_{\mathbf{D}}, y_{\mathbf{D}})$  to label the position of the brane whilst on the  $g = 0$  branches we shall use the notation  $(x, y)$  since the brane can be anywhere on the curve. When we approach certain boundaries of the moduli space we will be able to read off corresponding gauge dynamics.

The moduli space has boundaries when the brane (at  $\mathbf{D}$ ) approaches one of the punctures  $\mathbf{A}$ ,  $\mathbf{B}$  or  $\mathbf{C}$  and also when some of the moduli of the curve approach infinity.

If the brane approaches  $\mathbf{A}$  then this corresponds to the  $\mathbb{Z}_2$ -orbifold of deformed conifold with  $\mathbb{RP}^3$  growing large in the original IIA setup. When this happens on a  $g = 0$  branch we expect to find  $SU(N)$  gauge dynamics whilst on a  $g = 1$  branch we should find  $SU(N)$  broken by a Wilson line.

If  $\mathbf{D}$  approaches  $\mathbf{B}$  or  $\mathbf{C}$  this corresponds to the orbifold of resolved conifold with a large  $S^2$  in the original IIA framework with large  $\mathbb{P}^1$ . As we have discussed this can lead to  $SU(2)$  or trivial gauge dynamics from the  $\mathbb{R}^4/\mathbb{Z}_2$  singularity. We shall see that such limits of moduli space can also occur on the  $g = 1$  branches and correspond to  $SU(2)$  broken by Wilson lines. The possibility of including such Wilson lines is easy to understand from the M-theory picture where the  $SU(2)$  theory is realized on  $S^3/\mathbb{Z}_N$ .

Finally, if some of the moduli of the curve approach infinity on a  $g = 1$  branch, we expect this to describe a limit in which  $\mathbb{P}^1 \times \mathbb{P}^1$  grows large in the original IIA setup.

For example on the  $g = 0$  branch, let the brane approach the point  $\mathbf{A}$ . Since the  $g = 0$  branch has no low-energy  $U(1)$  gauge dynamics, the  $SU(N)$  dynamics should be encoded near the puncture  $\mathbf{A}$ . In this region, the curve becomes approximately

$$2P(1)y = (1 - x)^N. \quad (5.18)$$

$P(1)$  is nonzero, by equation (5.12) and one can regard this as expressing the  $SU(N)$  dynamics by identifying  $y$  with the SYM scale and  $1 - x$  as the gaugino condensate. One can read off the SYM dynamics from other punctures in a similar way as long as the curve is not singular there.

Let us now analyze the cases of small  $N$  one by one, starting with  $N = 1$ .

### N=1

In this case  $P(x)$  is of degree zero, so it is a constant  $P(x) = P(0) = 1$ . We have only one  $g = 0$  branch given by

$$\hat{y}^2 = (y - 1)^2 = x. \quad (5.19)$$

This case is better understood by going back to M-theory and choosing the M-theory circle from the second  $SU(2)$  factor  $g_2$ . The semiclassical region 2, which is centered at the puncture **B**, then corresponds to two D6-branes wrapped on a large  $S^3$  of the deformed conifold. The phases 1, 3 are centered at **A,C** and correspond to the resolved conifold with a large  $S^2$  and flux.

### N=2

In this case there are two sign choices for  $P_1(x)$ ,  $P_1(x) = 1 \mp x$ . Correspondingly there are two curves of genus zero,

$$\begin{aligned} (-) \quad \hat{y}^2 &= (y - 1 + x)^2 = 0, \\ (+) \quad y^2 - 2y(1 + x) + (1 - x)^2 &= 0. \end{aligned} \quad (5.20)$$

For the  $(-)$  choice the IIB target space becomes just the line of  $A_1$  singularity. The other choice agrees with (5.15), and we claim that it describes the quantum moduli space of vacua for  $N = 2$ .

### N=3

In this case  $P_1(x) = 1 + sx$  has one modulus, and we have a one-parameter family of curves of  $g = 1$ ,

$$\hat{y}^2 = (1 + sx)^2 - (1 - x)^3 = x^3 + (s^2 - 3)x^2 + (2s + 3)x. \quad (5.21)$$

The three punctures **A,B,C** are at

$$(x_{\mathbf{A}}, \hat{y}_{\mathbf{A}}) = (1, -1 - s), \quad (x_{\mathbf{B}}, \hat{y}_{\mathbf{B}}) = (0, 0), \quad (x_{\mathbf{C}}, \hat{y}_{\mathbf{C}}) = (\infty, \infty),$$

The position of the free D5-brane **D** is easily obtained

$$x_{\mathbf{D}} = 2s + 3, \quad \hat{y}_{\mathbf{D}} = (s + 1)(2s + 3), \quad y_{\mathbf{D}} = 4(s + 1)^2. \quad (5.22)$$

This genus one curve should be identified with the branch  $(N_+, N_-) = (1, 2)$ . From the relation between the moduli of the curve and the Kähler parameters of the GLSM, one finds that the local  $\mathbb{WP}_{3,1,2}^2$  becomes large in the IIA side as  $s \rightarrow \infty$  and  $\mathbf{D}$  approaches **C**. The curve degenerates to  $g = 0$  for the following values of  $s$  and  $x_{\mathbf{D}}$ ;

$$\begin{aligned} s = 3, \quad (x_{\mathbf{D}}, y_{\mathbf{D}}) &= (9, 64), \quad \hat{y}^2 = x(x+3)^2, \\ s = -1, \quad (x_{\mathbf{D}}, y_{\mathbf{D}}) &= (1, 0), \quad \hat{y}^2 = x(x-1)^2, \\ s = -\frac{3}{2}, \quad (x_{\mathbf{D}}, y_{\mathbf{D}}) &= (0, 1), \quad \hat{y}^2 = x^2(x-\frac{3}{4}). \end{aligned} \quad (5.23)$$

The first choice of  $s$  agrees with (5.15), so it should correspond to the branch with trivial Wilson line. The semiclassical points 1,2,3 of figure 1 are identified with  $x_{\mathbf{D}} = 1, 0, \infty$  or  $\mathbf{D}$  approaching one of the punctures. The other two curves of genus zero are singular, one at  $(x, y) = (1, 0)$  and the other at  $(0, 1)$ , as explained in the previous subsection. They both correspond to  $\mathbf{D}$  approaching the punctures **A** and **B**, and are at the boundary of the  $g = 1$  branch.

The geometric transition involving a non-trivial Wilson line on the D6-branes wrapped on  $\mathbb{RP}^3$  should be described by the family of  $g = 1$  curves. In particular, the coordinates  $(x_{\mathbf{D}}, y_{\mathbf{D}})$  are related to the disc instanton factors in the GLSM picture in the  $g = 1$  branch as well. They obey the equation

$$y_{\mathbf{D}} = (1 - x_{\mathbf{D}})^2. \quad (5.24)$$

Near the boundary  $(x_{\mathbf{D}}, y_{\mathbf{D}}) = (1, 0)$  one can read off the  $SU(2) \times U(1)$  SYM dynamics corresponding to  $SU(3)$  gauge symmetry with a nontrivial  $\mathbb{Z}_2$  Wilson line. The other boundary  $(x_{\mathbf{D}}, y_{\mathbf{D}}) = (0, 1)$  corresponds to the classical  $SU(2)$  gauge symmetry broken by a  $\mathbb{Z}_3$  Wilson line.

## N=4

In this case there are two one-parameter families for  $P_2(x)$ ,  $P_2(x) = 1 + sx \pm x^2$ . We will study both choices in detail, and try to read off the correct number of vacua for each theory.

For (+) choice we have a family of  $g = 1$  curves

$$\hat{y}^2 = (1 + sx + x^2)^2 - (1 - x)^4 = (s + 2)\{2x^3 + (s - 2)x^2 + 2x\}, \quad (5.25)$$

with **A,B,C,D** at

$$(x_{\mathbf{A}}, \hat{y}_{\mathbf{A}}) = (1, -s - 2), \quad (x_{\mathbf{B}}, \hat{y}_{\mathbf{B}}) = (0, 0), \quad (x_{\mathbf{C}}, \hat{y}_{\mathbf{C}}) = (\infty, \infty), \quad (x_{\mathbf{D}}, \hat{y}_{\mathbf{D}}) = (1, s + 2).$$

This family of  $g = 1$  curves should describe one of the  $(N_+, N_-) = (2, 2)$  branches. Note that  $x_{\mathbf{D}} = 1$  everywhere on this branch. If we are in the vacua where the values of the

gaugino condensate for the two  $SU(2)$  factors are of opposite sign, then the sum of the two  $SU(2)$  gaugino condensates vanishes irrespective of the value of the gauge coupling. This suggests that we interpret  $1 - x_{\mathbf{D}}$  as the sum of the gaugino condensates. We will find a similar result when we study  $N = 5$  at an  $SU(2) \times SU(3)$  point.

The  $g = 1$  curve degenerates to  $g = 0$  at two points,

$$\begin{aligned} s = 6, \quad (x_{\mathbf{D}}, y_{\mathbf{D}}) &= (1, 16), \quad \hat{y}^2 = 16x(x+1)^2, \\ s = -2, \quad (x_{\mathbf{D}}, y_{\mathbf{D}}) &= (1, 0), \quad \hat{y}^2 = 0. \end{aligned} \quad (5.26)$$

The first one agrees with the M-theory curve of  $g = 0$ , and it should be identified with the branch with trivial Wilson line. The latter is the case where the target space becomes a line of  $A_1$  singularities.

For  $(-)$  choice we have a family of  $g = 1$  curves

$$\hat{y}^2 = (1 + sx - x^2)^2 - (1 - x)^4 = (-2s + 4)x^3 + (s^2 - 8)x^2 + (2s + 4)x, \quad (5.27)$$

with **A,B,C,D** at

$$(x_{\mathbf{A}}, \hat{y}_{\mathbf{A}}) = (1, -s), \quad (x_{\mathbf{B}}, \hat{y}_{\mathbf{B}}) = (0, 0), \quad (x_{\mathbf{C}}, \hat{y}_{\mathbf{C}}) = (\infty, \infty), \quad (x_{\mathbf{D}}, \hat{y}_{\mathbf{D}}) = \left(\frac{2+s}{2-s}, \frac{s(2+s)}{2-s}\right).$$

One can also find a strange relation between  $x_{\mathbf{D}}$  and  $y_{\mathbf{D}}$ :

$$y_{\mathbf{D}} = -\frac{2s^3}{(2-s)^2} = \frac{(1-x_{\mathbf{D}})^3}{1+x_{\mathbf{D}}}.$$

This family degenerates to  $g = 0$  at three points,

$$\begin{aligned} s = 0, \quad (x_{\mathbf{D}}, y_{\mathbf{D}}) &= (1, 0), \quad \hat{y}^2 = 4x(x-1)^2, \\ s = -2, \quad (x_{\mathbf{D}}, y_{\mathbf{D}}) &= (0, 1), \quad \hat{y}^2 = 4x^2(2x-1), \\ s = 2, \quad (x_{\mathbf{D}}, y_{\mathbf{D}}) &= (\infty, \infty), \quad \hat{y}^2 = 4x(2-x). \end{aligned} \quad (5.28)$$

These degenerations all correspond to the boundary of the moduli space where **D** approaches one of the three punctures, and they are all singular. There is therefore no  $g = 0$  branch connected to this  $g = 1$  branch.

Let us count the number of vacua for some semi-classical regions of the  $g = 1$  branch where the microscopic theory is a  $\mathcal{N} = 1$  SYM theory. First, near  $(x_{\mathbf{D}}, y_{\mathbf{D}}) = (1, 0)$  the UV theory is  $SU(2) \times SU(2) \times U(1)$  SYM theory which has four vacua. For each small value of  $y_{\mathbf{D}}$  there is a single value of  $x_{\mathbf{D}}$  on the  $(+)$  branch and three values of  $x_{\mathbf{D}}$  on the  $(-)$  branch. Secondly, near  $(x_{\mathbf{D}}, y_{\mathbf{D}}) = (0, 1)$  the UV theory should be a seven-dimensional  $SU(2)$  gauge theory compactified on  $S^3/\mathbb{Z}_4$  with a non-trivial  $\mathbb{Z}_4$  Wilson line. Note that such a Wilson line is unique up to conjugations by  $SU(2)$ . The corresponding vacuum can be found on the  $(-)$  branch and is the second line of (5.28). The argument proceeds in the same way for the third semi-classical region  $(x_{\mathbf{D}}, y_{\mathbf{D}}) = (\infty, \infty)$ , where the UV theory

is again seven-dimensional  $SU(2)$  gauge theory on  $S^3/\mathbb{Z}_4$  with a  $\mathbb{Z}_4$  Wilson line and the corresponding vacuum is the third line of (5.28).

## N=5

From here on we have to tune the moduli of the polynomial  $P_2(x) = 1 + s_1 x + s_2 x^2$  so that the curve has reduced genus  $g \leq 1$ . There are three one-parameter families of  $g = 1$  curves, two of which are singular at the punctures **A** and **B** respectively. The remaining one is given by

$$\begin{aligned}\hat{y}^2 &= \left(1 + \frac{-s^4 - 3s^3 + s^2 + 3s + 4}{2s}x + \frac{-3s^3 - 3s^2 - s + 1}{2s^2}x^2\right)^2 - (1 - x)^5 \\ &= (x + s^2 + 2s)^2 G_3(x), \\ G_3(x) &= x^3 + \frac{s^6 + 2s^5 - 5s^4 - 5s^2 - 2s + 1}{4s^4}x^2 + \frac{-s^2 + s + 1}{s^3}x.\end{aligned}\quad (5.29)$$

The semi-classical regions of  $g = 1$  branches labeled by  $(N_+, N_-) = (1, 4)$  and  $(3, 2)$  are identified with  $s \sim 0$  and  $s \sim \infty$ , respectively. This shows that the two classical  $g = 1$  branches are on the same branch of quantum moduli space. On the reduced curve  $\tilde{y}^2 = G_3(x)$  the three punctures are located at

$$(x_{\mathbf{A}}, \tilde{y}_{\mathbf{A}}) = (1, \frac{(s-1)(s+1)^2}{2s^2}), \quad (x_{\mathbf{B}}, \tilde{y}_{\mathbf{B}}) = (0, 0), \quad (x_{\mathbf{C}}, \tilde{y}_{\mathbf{C}}) = (\infty, \infty), \quad (5.30)$$

so the free D5-brane sits at

$$x_{\mathbf{D}} = \frac{-s^2 + s + 1}{s^3}, \quad \tilde{y}_{\mathbf{D}} = \frac{(s-1)(s+1)^2(s^2 - s - 1)}{2s^5}, \quad y_{\mathbf{D}} = \frac{(s-1)^4(s+1)^6}{s^8}. \quad (5.31)$$

Generically there are three values of  $s$  corresponding to a given  $x_{\mathbf{D}}$ , so this  $g = 1$  branch is covering the  $x_{\mathbf{D}}$ -space three times. Two of the three sheets meet at

$$x_{\mathbf{D}} = 1 \quad (s = 1, -1, -1), \quad x_{\mathbf{D}} = -\frac{5}{27} \quad (s = -\frac{3}{5}, 3, 3).$$

One finds  $(x_{\mathbf{D}}, y_{\mathbf{D}}) = (\infty, \infty)$  or  $(0, \infty)$  at the two large-volume points corresponding to  $(N_+, N_-) = (1, 4)$  or  $(3, 2)$ . Aside from them, the reduced curve degenerates to  $g = 0$  for the following values of  $s$  and  $x_{\mathbf{D}}$ :

$$\begin{aligned}s &= -2 \pm \sqrt{5}, & (x_{\mathbf{D}}, y_{\mathbf{D}}) &= (45 \pm 20\sqrt{5}, 62976 \pm 28160\sqrt{5}), & P_2(x) &= 1 + 10x + 5x^2, \\ s &= -1 & (x_{\mathbf{D}}, y_{\mathbf{D}}) &= (1, 0), & P_2(x) &= (1 - x)^2, \\ s &= 1 & (x_{\mathbf{D}}, y_{\mathbf{D}}) &= (1, 0), & P_2(x) &= (1 + 3x)(1 - x), \\ s &= \frac{1}{2}(1 \pm \sqrt{5}), & (x_{\mathbf{D}}, y_{\mathbf{D}}) &= (0, 1), & P_2(x) &= 1 - \frac{5}{2}x - \frac{5}{4}(1 \pm \sqrt{5})x^2.\end{aligned}\quad (5.32)$$

The first of these agrees with the M-theory  $g = 0$  curve and corresponds to the branch with trivial Wilson line. Interestingly, the  $g = 1$  branch meets this  $g = 0$  branch at two

different points. Near  $s = \pm 1$  on  $g = 1$  branch,  $(x_{\mathbf{D}}, y_{\mathbf{D}})$  approaches  $(1, 0)$ , so one should be able to read off the SYM dynamics from

$$y_{\mathbf{D}} = \frac{(s+1)^6(s-1)^4}{s^8}, \quad 1-x_{\mathbf{D}} = \frac{(s+1)^2(s-1)}{s^3}.$$

Near  $s = 1$  one can read off the  $SU(4)$  dynamics from the approximate relation  $4y_{\mathbf{D}} \simeq (1-x_{\mathbf{D}})^4$ . The situation is more interesting at  $s = -1$ . In this case  $y_{\mathbf{D}} \sim 16(s+1)^6$  and  $1-x_{\mathbf{D}} \sim 2(s+1)^2$  to leading order, so one can read off the  $SU(3)$  dynamics at this order. Including the next-to leading order terms one finds

$$1-x_{\mathbf{D}} \simeq 2\left(\frac{y_{\mathbf{D}}}{16}\right)^{\frac{2}{6}} + \left(\frac{y_{\mathbf{D}}}{16}\right)^{\frac{3}{6}},$$

so the six vacua of  $SU(3) \times SU(2)$  SYM theory can be read off correctly. Indeed this agrees with our earlier interpretation of  $1-x_{\mathbf{D}}$  as a sum of gaugino condensates for the two gauge groups. Finally, near  $s = \frac{1}{2}(1 \pm \sqrt{5})$  one obtains approximately linear relations between  $1-y_{\mathbf{D}}$  and  $x_{\mathbf{D}}$ , describing the  $SU(2)$  gauge symmetry broken by non-trivial  $\mathbb{Z}_5$  Wilson lines. The two values of  $s$  will correspond to two physically different Wilson lines,  $W = \exp(\frac{2\pi i \tau_3}{5})$  and  $W = \exp(\frac{4\pi i \tau_3}{5})$ .

## N=6

Let us first discuss the case with  $s_3 = +1$ ,  $P(x) = 1 + s_1x + s_2x^2 + x^3$ :

$$\begin{aligned} \hat{y}^2 &= (1 + s_1x + s_2x^2 + x^3)^2 - (1-x)^6 \\ &= x\{2 + (s_1 - 3)x + (s_2 + 3)x^2\}\{s_1 + 3 + (s_2 - 3)x + 2x^2\}. \end{aligned} \quad (5.33)$$

Since we do not want the degeneration of roots to occur at  $x = 0, 1, \infty$ , we discard the curves of  $g = 1$  given by  $s_1 = -3$ ,  $s_2 = -3$  or  $s_1 + s_2 = -2$ . There are thus two families of genus one curves defined by the conditions

$$(I) \quad s_2 = \frac{1}{8}(s_1 - 3)^2 - 3 \quad \text{or} \quad (II) \quad s_1 = \frac{1}{8}(s_2 - 3)^2 - 3. \quad (5.34)$$

We define the reduced curve for each branch as follows:

$$\begin{aligned} (I) \quad \tilde{y}^2 &= (s_1 + 3)x + (\frac{1}{8}(s_1 - 3)^2 - 6)x^2 + 2x^3, \\ (II) \quad \tilde{y}^2 &= (s_2 + 3)x^3 + (\frac{1}{8}(s_2 - 3)^2 - 6)x^2 + 2x. \end{aligned} \quad (5.35)$$

The location of the free D5-brane on the curve is given for each case by

$$\begin{aligned} (I) \quad x_{\mathbf{D}} &= \frac{s_1 + 3}{2}, \quad \tilde{y}_{\mathbf{D}} = \frac{(s_1 + 1)(s_1 + 3)}{4\sqrt{2}}, \quad y_{\mathbf{D}} = \frac{(s_1 + 1)^4}{16}, \\ (II) \quad x_{\mathbf{D}} &= \frac{2}{s_2 + 3}, \quad \tilde{y}_{\mathbf{D}} = \frac{s_2 + 1}{\sqrt{2}(s_2 + 3)}, \quad y_{\mathbf{D}} = \frac{(s_2 + 1)^4}{2(s_2 + 3)^3}. \end{aligned} \quad (5.36)$$

On each of these two branches  $(x_{\mathbf{D}}, y_{\mathbf{D}})$  obey

$$(I) \quad y_{\mathbf{D}} = (1 - x_{\mathbf{D}})^4, \quad (II) \quad y_{\mathbf{D}} = (1 - x_{\mathbf{D}})^4/x_{\mathbf{D}}. \quad (5.37)$$

So there are eight values of  $x_{\mathbf{D}}$  for each small value of  $y_{\mathbf{D}}$ , accounting for half the required vacua for the  $SU(N_+) \times SU(N_-)$  SYM theories with  $(N_+, N_-) = (4, 2)$  and  $(2, 4)$ . The limit  $s_1 \rightarrow \infty$  or  $(x_{\mathbf{D}}, y_{\mathbf{D}}) = (\infty, \infty)$  on (I) corresponds to a semi-classical limit with large  $\mathbb{WP}_{3,1,2}^2/\mathbb{Z}_2$ , and similarly  $s_2 \rightarrow \infty$  or  $(x_{\mathbf{D}}, y_{\mathbf{D}}) = (0, \infty)$  on (II) corresponds to another large  $\mathbb{WP}_{3,2,1}^2/\mathbb{Z}_2$ . There are also points  $(x_{\mathbf{D}}, y_{\mathbf{D}}) = (0, 1)$  on (I) and  $(x_{\mathbf{D}}, y_{\mathbf{D}}) = (\infty, \infty)$  on (II) corresponding to two different semi-classical points with  $SU(2)$  broken by a non-trivial  $\mathbb{Z}_6$  Wilson lines. However, there are two inequivalent  $\mathbb{Z}_6$  Wilson lines in  $SU(2)$  and we have recovered only one of them at each semiclassical point.

Besides these points, further degeneration to  $g = 0$  occurs at

$$\begin{aligned} (I) \quad & s_1 = 15, \quad (x_{\mathbf{D}}, y_{\mathbf{D}}) = (9, 4096), \quad P_3(x) = 1 + 15x + 15x^2 + x^3, \\ & s_1 = -1, \quad (x_{\mathbf{D}}, y_{\mathbf{D}}) = (1, 0), \quad P_3(x) = 1 - x - x^2 + x^3, \\ (II) \quad & s_2 = 15, \quad (x_{\mathbf{D}}, y_{\mathbf{D}}) = \left(\frac{1}{9}, \frac{4096}{729}\right), \quad P_3(x) = 1 + 15x + 15x^2 + x^3, \\ & s_2 = -1, \quad (x_{\mathbf{D}}, y_{\mathbf{D}}) = (1, 0), \quad P_3(x) = 1 - x - x^2 + x^3. \end{aligned} \quad (5.38)$$

The curve of genus zero with  $s_1 = s_2 = 15$  agrees with the M-theory curve, so it describes the  $g = 0$  branch of quantum moduli space. The two  $g = 1$  branches (I) and (II) are attached to two different points on the  $g = 0$  branch.

Let us next consider the case  $s_3 = -1$ ,  $P(x) = 1 + s_1x + s_2x^2 - x^3$ ;

$$\dot{y}^2 = x\{s_1 + 3 + (s_2 - 3)x\}\{2 + (s_1 - 3)x + (s_2 + 3)x^2 - 2x^3\} \quad (5.39)$$

We first look for curves with  $g = 1$ , excluding singular ones given by  $s_1 = -3$ ,  $s_2 = 3$  or  $s_1 + s_2 = 0$ . The degeneration of branching points of interest occurs only when the third factor in the right hand side develops a double root. Denoting the double root by  $s$  we immediately obtain

$$s_1 = -2s^2 + 3 - \frac{4}{s}, \quad s_2 = 4s - 3 + \frac{2}{s^2}. \quad (5.40)$$

The location of the free D5-brane is given by

$$x_{\mathbf{D}} = \frac{s+2}{s(2s+1)}, \quad y_{\mathbf{D}} = \frac{16(1-s)^3(1+s)^5}{s^4(2s+1)^3}, \quad (5.41)$$

The semi-classical points of the  $g = 1$  branch are identified with  $s = 0, \infty$  and  $(x_{\mathbf{D}}, y_{\mathbf{D}}) = (\infty, \infty)$ . Degeneration to  $g = 0$  occurs at

$$\begin{aligned} s = 1, \quad & (x_{\mathbf{D}}, y_{\mathbf{D}}) = (1, 0), \quad P_3(x) = (1 - x)^3, \\ s = -1, \quad & (x_{\mathbf{D}}, y_{\mathbf{D}}) = (1, 0), \quad P_3(x) = (1 - x)(1 + 6x + x^2), \\ s = -2, \quad & (x_{\mathbf{D}}, y_{\mathbf{D}}) = (0, 1), \quad P_3(x) = 1 - 3x - \frac{21}{2}x^2 - x^3, \\ s = -1/2, \quad & (x_{\mathbf{D}}, y_{\mathbf{D}}) = (\infty, \infty), \quad P_3(x) = 1 + \frac{21}{2}x + 3x^2 - x^3. \end{aligned} \quad (5.42)$$

They are all singular at one of the punctures. Again, for the sign choice of  $s_3 = (-)$  there is no  $g = 0$  branch connected to the  $g = 1$  branch.

Using (5.41) one can easily check that, near  $(x_{\mathbf{D}}, y_{\mathbf{D}}) = (1, 0)$ , there are eight values of  $x_{\mathbf{D}}$  for each fixed  $y_{\mathbf{D}}$  (three are near  $s = 1$  and five are near  $s = -1$ ). Also, near each of  $(x_{\mathbf{D}}, y_{\mathbf{D}}) = (0, 1)$  and  $(\infty, \infty)$  there is one vacuum corresponding to a non-trivial  $\mathbb{Z}_6$  Wilson line. All the semi-classical vacua with a  $U(1)$  in the IR were thus identified with the special points on the  $g = 1$  branch.

### Acknowledgments

We wish to thank R. Dijkgraaf, J. Gomis, A. Hanany, M. Herbst, T. Hirayama, M. Jinzenji, S. Kadir, K. Kennaway, S. Minabe, T. Okuda, J. Park, A. Peet, E. Poppitz, S. Rinke, A. Takahashi and especially K. Hori for useful discussions and comments. KH was supported in part by NSERC of Canada, and DCP was funded by PREA of Ontario.

## References

- [1] C. Vafa, J. Math. Phys. **42**, 2798 (2001).
- [2] R. Gopakumar and C. Vafa, Adv. Theor. Math. Phys. **3**, 1415 (1999).
- [3] B. S. Acharya, arXiv:hep-th/0011089.
- [4] M. Atiyah, J. M. Maldacena and C. Vafa, J. Math. Phys. **42**, 3209 (2001).
- [5] M. Atiyah and E. Witten, Adv. Theor. Math. Phys. **6**, 1 (2003).
- [6] T. Friedmann, Nucl. Phys. B **635**, 384 (2002).
- [7] H. Ita, Y. Oz and T. Sakai, JHEP **0204**, 001 (2002).
- [8] F. Cachazo, N. Seiberg and E. Witten, JHEP **0302**, 042 (2003).
- [9] F. Cachazo, N. Seiberg and E. Witten, JHEP **0304**, 018 (2003).
- [10] M. Aganagic, A. Klemm, M. Marino and C. Vafa, JHEP **0402**, 010 (2004).
- [11] T. Okuda and H. Ooguri, Nucl. Phys. B **699**, 135 (2004).
- [12] M. Aganagic and C. Vafa, JHEP **0305**, 061 (2003).
- [13] A. Brandhuber, J. Gomis, S. S. Gubser and S. Gukov, Nucl. Phys. B **611**, 179 (2001).
- [14] L. A. Pando Zayas and A. A. Tseytlin, Phys. Rev. **D63**, (2001).
- [15] M. Cvetic, G. W. Gibbons, H. Lu and C. N. Pope, Phys. Lett. B **534**, 172 (2002).
- [16] N. C. Leung and C. Vafa, Adv. Theor. Math. Phys. **2**, 91 (1998).
- [17] M. Aganagic and C. Vafa, arXiv:hep-th/0012041.
- [18] M. Aganagic, A. Klemm, M. Marino and C. Vafa, arXiv:hep-th/0305132.
- [19] M. Aganagic, A. Klemm and C. Vafa, Z. Naturforsch. A **57**, 1 (2002).
- [20] P. Griffiths and J. Harris, “Principles of Algebraic Geometry,” John Wiley & sons, Inc.
- [21] K. Hori and C. Vafa, arXiv:hep-th/0002222.
- [22] K. Hori, A. Iqbal and C. Vafa, arXiv:hep-th/0005247.

- [23] A. Strominger, Nucl. Phys. B **451**, 96 (1995).
- [24] B. R. Greene, D. R. Morrison and A. Strominger, Nucl. Phys. B **451**, 109 (1995).